Functional Characterization of Peripheral Immune Cells in BAMBI *knockout* mice.

Master's Thesis

Oliver Adrián Caballero López

Director: Luis Gil De Gómez Sesma

Co-Director: Ramón Merino Pérez

Interuniversity Master's Degree in Molecular Biology and Biomedicine

Laboratory of Immunopathology/Department of Molecular Biology/University of Cantabria

Santander, June 2024.

Index.

1. Background. 1

1.1. Spleen: structure and function. 1

1.2. T lymphocytes: development, characteristics, and function. 2

1.3. Natural Killer Cells: development, characteristics and function. 6

1.4. Transforming Growth Factor-β (TGF-β). 7

1.5. BAMBI. 9

2. Objectives. 12

2.1. General objective. 12

2.2. Specific objectives. 12

3. Materials and methods. 13

3.1. Animals. 13

3.3. Characterization of Spleen T cell and NK cell populations. 13

3.4. Gating strategy 15

3.5. CD4+ T cell purification. 18

3.6. CD8+ T cell purification. 18

3.7. Purification of NK cells. 19

3.8. Spontaneous cell death. 20

3.9. CD4+ and CD8+ T cell proliferation assay. 20

3.10. *Ex vivo* cytotoxicity assay of murine NKs cells. 21

4. Results 25

4.1. Phenotypic characterization of lymphocyte and NK cell populations in the spleen of BAMBI-KO mice. 25

4.2. Effect of BAMBI on spontaneous cell death of peripheral T lymphocytes. 31

4.3. The lack of BAMBI expression increases cell proliferation of peripheral CD4+ and CD8+ T lymphocytes. 32

4.4. The absence of BAMBI causes an increase in NK cell-mediated cytotoxicity. 33

5. Discussion 36

6. Conclusions. 39

7. Bibliography. 40

1. Background.

1.1. Spleen: structure and function.

The spleen is an organ located in the abdomen, directly below the diaphragm and is connected to the stomach. It is considered the first and largest blood filter in the body. In essence, the spleen is organized as a branching network of arterial vessels, where the smallest arterioles end in a sinusoidal venous system. The organ is surrounded by a fibrous layer of connective tissue, called capsule, from which arise the trabeculae that support the larger vasculature (Steiniger & Barth, 2000).

The spleen is divided into red pulp and white pulp. These regions have different functions and structures and between them there is an area called perifollicular (in humans) and marginal (in rodents) (**Figure 1**). The red pulp is responsible for extracting old, dead and/or opsonized cells from the bloodstream. This function is carried out by macrophages located in the cords, which consist of fibroblasts and reticular fibers and form an open blood system without an endothelial lining (Lewis et al., 2019). Ageing erythrocytes cannot overpass those cords since they have stiffening membranes and thus are phagocytosed by the red-pulp macrophages. The red pulp also has a variety of leukocytes with innate functions, including neutrophils, monocytes, dendritic cells, and macrophages (Nolte et al., 2000). In the red pulp we can find plasmablasts and plasma cells, differentiated B lymphocytes that come from the follicles of the white pulp after antigen-specific differentiation. These cells are in charge of release rapidly antibodies in the bloodstream. On the other hand, in the white pulp there are two different zones: the T cell zone and the B cell zone (follicles) and the perifollicular (or marginal) zone. The follicular zone has T and B cell compartments around the branching arterial vessels. The organization of the follicular zone is controlled by specific chemokines that attract T and B cells to their domains. In the T cell zone, T cell interact with dendritic cells (DCs), whereas in the B cell zone, there is a clonal expansion of activated B cells (Mebius & Kraal, 2005). However, the perifollicular (or marginal) zone contains a different type of innate B cell (the B cells of the marginal zone) that have the function of acting as a natural link between the innate and adaptative immune systems. In addition, at the interface between the red and white pulp, there are DCs and B cells of the marginal zone that have the function of catching antigens transported in the blood to the white pulp for surveillance by T and B cells (Calabro et al., 2016; Lu et al., 2017).

The spleen is an important organ for immune homeostasis due to the innate and adaptative responses. The white pulp has an exclusive adaptative response, whereas the perifollicular zone is involved in both innate and adaptative immunity. The innate immune response is due the presence of cells that express patterns-recognition

receptors (such as Toll-like receptors (TLRs)), C-type lectin SIGNR1, the type I scavenger receptor MARCO, etc. Instead, the adaptative immune response is due the entry of professional antigen-presenting cells (APCs) to the white pulp. Upon the entry of activated APCs to the white pulp, both T and B cells become activated and migrate to the edge of the B cell follicles where they interact (Mebius & Kraal, 2005).

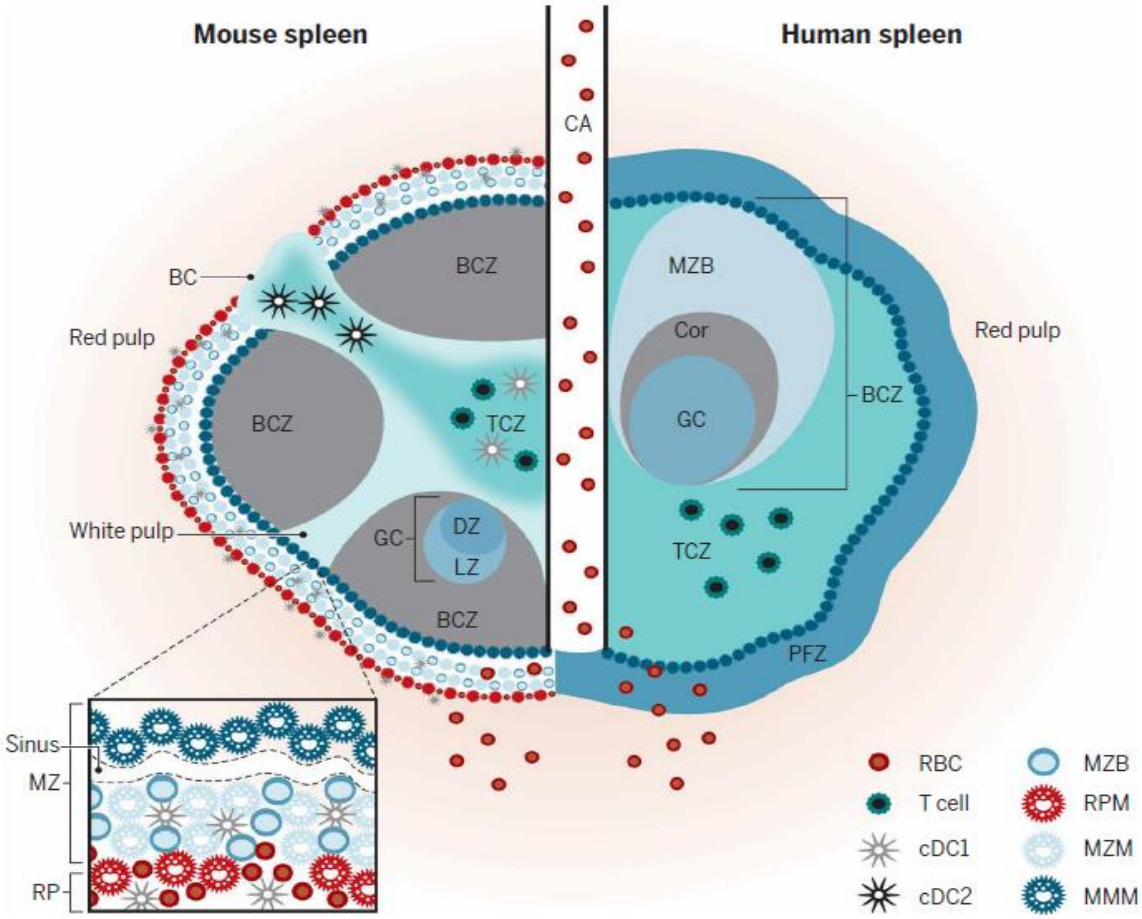

Figure 1. Cellular structure of mouse and human spleen. **Taken from Lewis, SM et al; 2019.* **RBC**: Red blood cells; **cDC 1&2:** dendritic cells; **MZB:** marginal zone B-cell; **RPM:** red pulp macrophages; **MZM:** marginal zone macrophages; **MMM:** marginal metalophilic macrophages; **TCZ:** T-cell zone; **GC:** germinal center; **BCZ**: B-cell zone; **RP**: red pulp; **MZ**: marginal zone; **DZ**: dark zone; **LZ**: light zone; and **PFZ**: perifollicular zone.

1.2. T lymphocytes: development, characteristics, and function.

T cells are the main effectors in the adaptive immune response against pathogens. These cells express an antigen receptor (TCR) that is clonally distributed and highly polymorphic. The TCR allows them to recognize a single antigen per T cell clone. After antigen recognition, T cells undergo clonal expansion, and thus acquiring effector functions. One of these functions is the production of cytokines in a paracrine way. The release of them activates other cells of the immune system to rid infected cells with high

precision (Fabbri, 2003).

T cells derive from lymphoid precursors that are produced in the bone marrow and differentiated in the thymus. The bone marrow progenitors lacking CD4+ and CD8+ coreceptors undergo the rearrangement of the *tcr* gene to generate CD4+CD8+ double-positive (DP) thymocytes. In the outer cortex of the thymus, DP thymocytes undergo a positive selection where DP cells that express the TCR with suitable affinity to bind the major histocompatibility complex (MHC) present in the cortical epithelial cells are selected to survive and mature. Next, in the inner cortex T cells undergoes a negative selection. During negative selection, immature T lymphocytes that recognize self-antigens presented strongly by DCs are eliminated or induced to undergo apoptosis (programmed cell death). Concurrently, T cells cease to express one of the two co-receptor molecules, becoming either CD4+ or CD8+ single-positive thymocytes. T cells that reach this phase migrate to the medulla of the thymus. In the medulla, the thymus epithelial cells (TEC) and medullary dendritic cells (mDCs) developed an important role in the presentation of antigens to the developing T cells. This process of antigen presentation in the thymus medulla is essential to ensure that only T cells with appropriate TCR are released into the periphery contributing to a functional immune system and avoiding autoreactivity. TCR is expressed on the cell surface as a complex with CD3 molecules that provide the signaling components and together exert their function by the specific recognition of foreign antigens that are processed and presented as peptides in MHCs expressed in the plasma membrane of APCs (Klein et al., 2014; Viret & Janeway, 1999). **Figure 2** shows the process that T lymphocytes undergo to reach the mature stage, from the hematopoietic stem cell in the bone marrow to the mature T lymphocytes in the peripheral lymphoid organs.

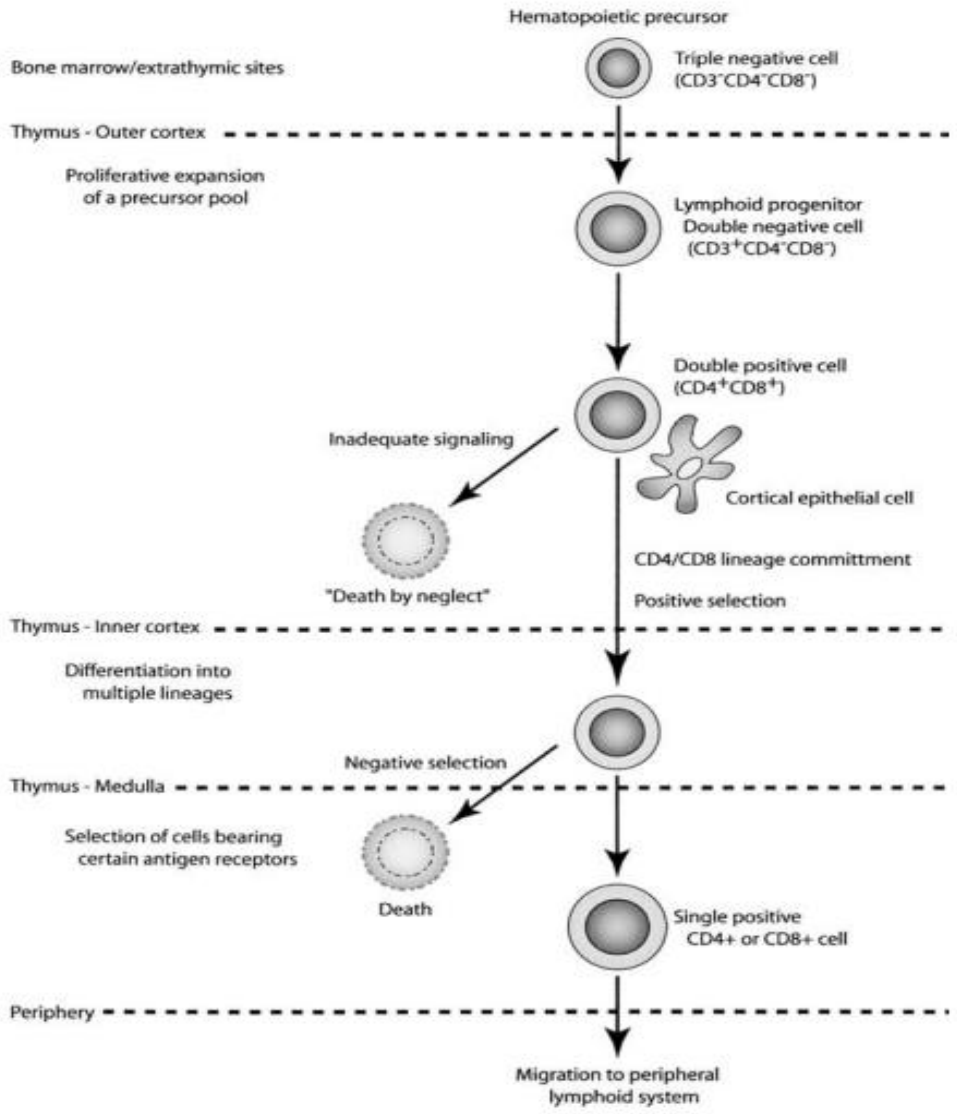

Figure 2. Development of T lymphocytes. **Taken from Vallejo AN et al; 2004.*

Upon antigen recognition and in the presence of costimulatory signals, T cells initiate interleukin-2 (IL-2) synthesis as well as transiently expression of high affinity receptor for IL-2 (IL2Rα or CD25). CD25 binds to other IL-2 receptor chains, which are the β chain (CD122) and the γ common chain (CD132) which does not participate in signaling. However, it increases the affinity for IL-2 by 10 to 100 times. IL-2 acts as an autocrine and paracrine growth factor, which produces clonal expansion of T cells with identical TCRs to the original. After the activation and expansion processes, there is a death phase where approximately 90% of the effector cells are eliminated by apoptosis using the mechanisms of Fas-FasL, tumor necrosis factor (TNF) and their receptors (TNFR I and II), as well as CD40-CD40L (Boyman & Sprent, 2012; Malek & Bayer, 2004).

There are different ways to expand and proliferate T cells *in vitro*. One of the most effective and widely described is using anti-CD3 antibodies immobilized on a surface

(culture plate) with either immobilized or soluble anti-CD28 antibodies. The simultaneous utilization of these two antibodies in T cell cultures provides them with the signal 1 and the costimulatory signal 2 that are indispensable for their proliferation (Levine et al., 1997).

T cells are divided into two main groups, CD4+ and CD8+ T cells. CD4+ T cells have different subpopulations that are determined by the nature and concentration of the antigen, the type of APC and its activation state, the environment of cytokines, and costimulatory molecules. CD4+ T cells, also known as T helper (Th) cells, have multifaceted stimulating roles towards other lymphocytes subtypes such as memory CD8+ cells and B cells to generate antibodies (Cano & Lopera, 2013). **Figure 3** shows the subpopulations of CD4+ T cells and the profile of cytokines secreted by each of them.

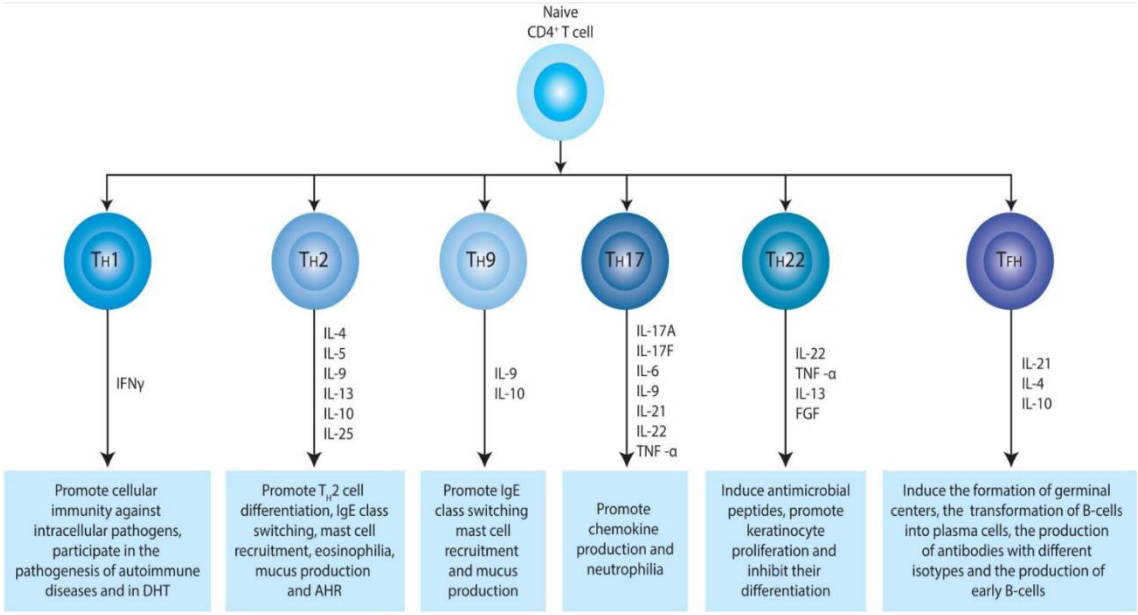

Figure 3. CD4+ T cell subpopulations and their cytokine profiles. **Taken from Cano & Lopera, 2013.*

On the other hand, CD8+ T cells have mainly a cytotoxic function, where these cells attack directly target cells including virus-infected cells or cancer cells (Cox et al., 2013). These cells induce apoptosis in target cells via release of killer granules or through expression of death ligands such as FasL (CD95). These granules contain perforins, granzymes, granulolysins, perforin inhibitors (which protect the lymphocyte from autolysis), and FasL (Lieberman, 2003). In addition, cytotoxic T lymphocytes release interferon-γ (IFN-γ) and TNF-α, which are important in the defense against viral infections and controlling tumor cell proliferation (Cox et al., 2013).

T cell differentiation occurs in three phases: clonal expansion, in which T cells differentiate into effector T cells; contraction, in which effector T cells die by apoptosis

and a memory phase, in which a fraction of T cells persists as memory T cells that protect against another infection. Memory T cells are the major circulating population in the blood. These cells are divided into central memory ($CD62L^+$, $CD44^+$), effector memory ($CD62L^-$, $CD44^+$) and stem-cell memory ($CD45RA^+$, $CCR7^+$, $CD95^+$ and $CD122^+$). Central memory and effector memory T cells can produce IL-2 and effector cytokines upon be stimulated. However, central memory T cells have a high proliferative ability whereas effector memory T cells produce more effector cytokines (Kumar et al., 2018).

1.3. Natural Killer Cells: development, characteristics and function.

Natural killer cells (NK cells) are the third largest lineage of lymphocytes present in the body. They are classified as cells of the innate immune system due to, unlike T and B cells, NK cells lack a single a single antigen recognition receptor allowing them to respond quickly against target cells in antigen non-specific manner (Borghesi et al., 2004; Di Santo, 2006).

NK cells derive from lymphoid progenitor cells present in the bone marrow, where the upregulation of certain transcription factors such as inhibitor of DNA binding 2 (ID2) and nuclear factor interleukin 3 regulated (E4BP4, known as NFIL3) and the depletion or absence of the zinc-finger transcription factor Bcl11b predispose to progenitors of the NK cell lineage. In the same way, these progenitor cells need a bone marrow microenvironment with stromal cells to generate mature NK cells (Sun JC & Lanier, 2011). NK cells are selected through the binding of their receptors to several MHC class I ligands. This positive selection is developed in the bone marrow by stromal and hematopoietic cells via killer immunoglobin-like receptors (KIRs), and the number of interactions between them establish the degree of responsiveness. KIRs are expressed during the development of NK cells and are responsible for establishing efficient systems that do not recognize self-antigen (Ljunggren & Kärre, 1990).

NK cells require mainly the presence of IL-15 for their maintenance and survival. IL-15 also plays an important role during the development of these cells. This interleukin increases the expression and activity of B-cell lymphoma 2 (BCL-2) and its family members in NK cells (Ma et al., 2006). At the same time, it inhibits the activity of the transcription factor forhead box O3A (FOXO3A) and the pro-apoptotic factor Bcl-2 interacting mediator of cell death (BIM) (Huntington et al., 2007). NK cells require certain signals for their activation and proliferation. One of these signals is the recognition of the cognate antigen via the LY49H activating receptor on NK cells (Dorner et al., 2004). However, it remains uncertain whether co-stimulatory signals such as CD28 is necessary for the effector activity *in vivo* during viral infection. Additionally, the secretion of IFN-γ and TNF, but not IL-2, depends on a "signal 3" produced by dendritic cells, which are: IL-12 and IFN-I (Andoniou et al., 2005) (**Figure 4**).

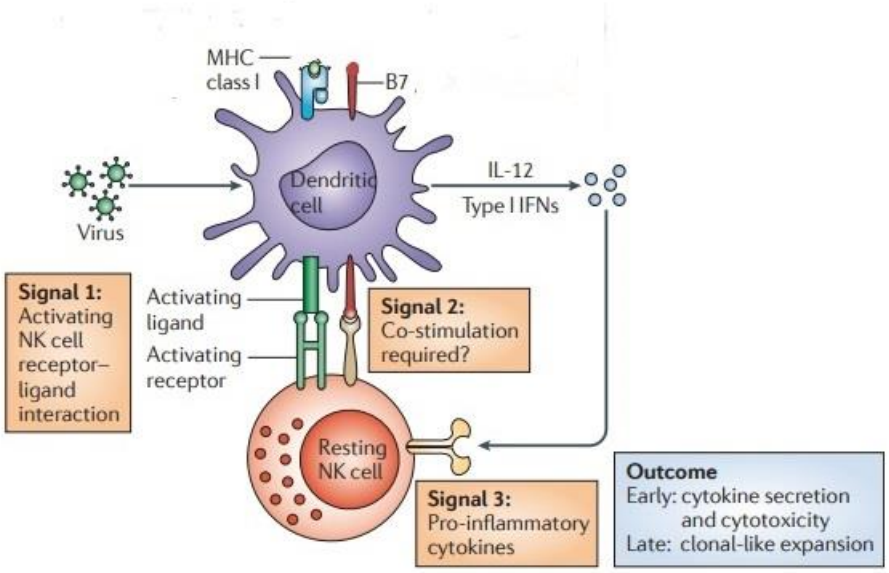

Figure 4. NK cell activation signals. **Modified from Sun JC & Lanier LL; 2011.*

The activation of NK cells and their activity can be studied using poly I:C (polyinosinic-polycytidylic) for the in *vivo* activation of NK cells. Poly I:C is a double-stranded RNA that is recognized by melanoma-differentiation associated gene 5 (MDA5) and TLR3 of NK cells. Upon recognition of the poly I:C by these receptors, NK cells are activated (Miyake et al., 2009). Once NK cells are activated *in vivo*, it is possible to study their cytotoxic activity in an *ex vivo* model using flow cytometry with CFSE/7-AAD (carboxyfluorescein succinimidyl ester/7-aminoactinomycin D). Once target cells (e.g., tumor cells) are labeled with CFSE, they are mixed with the NK cells and incubated together for a minimum of 4 hours where the cytotoxic activity of NK cells occurs. After this incubation and prior to analysis, the mixture of cells is labeled with 7-AAD. The percentage of CFSE-labeled target cells that were lysed by is determined by staining with 7-AAD and CFSE (Jung et al., 2021).

1.4. Transforming Growth Factor-β (TGF-β).

The transforming growth factor-β (TGF-β) family in humans includes 33 genes that code for a homodimeric or heterodimeric cytokine, which is secreted by different cell types. These proteins are synthesized as a precursor which is subsequently cleaved, thus generating the dimeric mature form that is linked through a disulfide bridge (Heldin & Moustakas, 2016). Members of the TGF-β family include molecules, such as, activins, Bone Morphogenetic Proteins (BMPs), Growth Differentiation Factors (GDFs), Müllerian Inhibiting Substance (MIS) and TGF-βs (TGF-β1, -β2, -β3, etc.).

TGF-β signaling is initiated by its receptor located on the plasma membrane of the cell. The TGF-β receptor (TGFR-β) has intrinsically dependent ATP (adenosine

triphosphate) proteinkinase activity with specificity mainly in tyrosine and threonine residues of certain proteins. TGF-β1, -β2, and -β3 are recognized by TGFR-β type I and II that are expressed in all cell types (Heldin & Moustakas, 2016). Upon ligand binding, TGFR-β type II phosphorylates and activates TGFR-β type I. On the other hand, TGFR-β type I phosphorylates and activates the receptor-activated SMADs (R-SMADs): SMAD2 and SMAD3. After activation of R-SMAD, it dissociates from the TGFR-β type I to subsequently form a complex with SMAD4. This complex is translocated to the cell nucleus where it associates with DNA-binding high-affinity transcription factors and chromatin remodeling proteins to up- or downregulate the expression of target genes. SMAD7, unlike the others SMAD, has an inhibitory activity. Thus, SMAD7 competes with R-SMADs for interaction with TGFR-β type I, as well as inhibits the activity of the SMAD complex in the cell nucleus (Tzavlaki & Moustakas, 2020) (**Figure 5**).

Additionally, there are non-canonical signaling pathways that involves proteins such as: Ras-Rho GTPases and Mitogen Activated Protein (MAPs) kinases, which are activated by TGF-β (Hartsough & Mulder, 1995; Mulder & Morris, 1992).

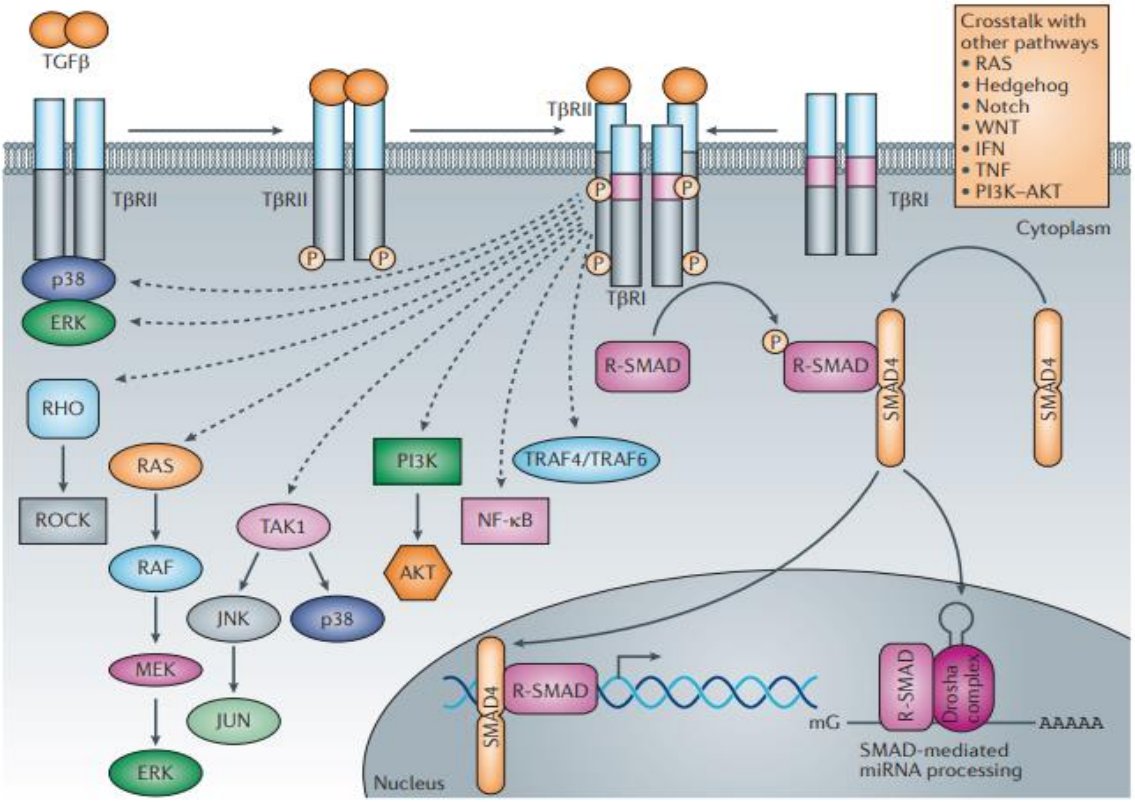

Figure 5. TFG-β signaling. Canonical and non-canonical path. **Taken from Akhurst R & Hata A; 2012.*

TGF-β has a suppressive activity in most immune cell precursors, especially T and B cells. In addition, it could influence their differentiation. For example, TGF-β up-regulates the expression of the transcription factor forkhead box protein P3 (*FoxP3*) in CD4+ T cells which leads them towards differentiation into regulatory T cells (Tregs). Additionally, TGF-β inhibits the differentiation of pro-inflammatory Th1 and Th2 cells and the production of IFN-γ by NK cells. In mice *TGF-β*$^{-/-}$, a hyperinflammatory phenotype is present due to aberrant activation of effector CD8+ and CD4+ T cells and Treg cell deficiency (Akhurst & Hata, 2012).

On the other hand, in certain conditions TGF-β has a pro-inflammatory role as well. Hence, in presence of IL-6, TGF-β produces the differentiation of CD4+ T cells towards Th17 cell line. Th17 has been linked to different inflammatory diseases, such as: psoriasis, systemic lupus erythematosus, asthma, and other autoimmune diseases (Bettelli et al., 2006).

1.5. BAMBI.

Bone Morphogenetic proteins and Activin Membrane Bound Inhibitor (BAMBI) is a transmembrane protein of 260 amino acids that has an extracellular domain. BAMBI is highly related to TGF-β type I receptor (TGF-βRI), but unlike other TGF-βRs, the intracellular domain does not have a serine/threonine kinase domain (Onichtchouk et al., 1999). BAMBI inhibits BMP and TGF-β-mediated gene transcription. It also inhibits TGF-β-induced phosphorylation of R-Smad. In addition, BAMBI blocks the formation of TGRF-β type I and II complexes and their signaling (Yan et al., 2009). Its expression is upregulated by TGF-β, BMP and β-catenin signaling due the binding to BAMBI transcriptional promoter trough SMAD3 and SMAD4 (Sekiya, Adachi et al., 2004; Sekiya, Oda et al., 2004). Instead, it is downregulated by the binding of lipopolysaccharide (LPS), an endotoxin which is the major component of external membrane of Gram negative bacteria, to CD14 at the plasma membrane, leading to activation of signaling via TLR4 that, ultimately, induces the MyD88/NF-κB signaling cascade (Seki et al., 2007). The **Figure 6** shows the signaling pathways regulated by BAMBI and its role in gene expression.

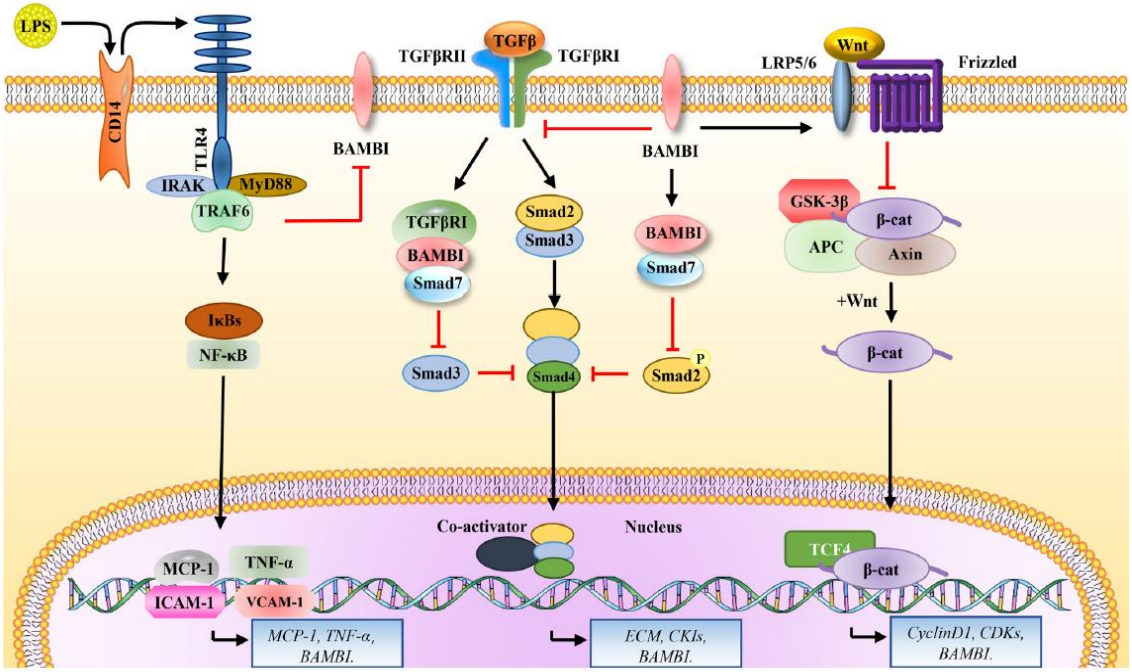

Figure 6. Signaling pathways regulated by BAMBI. **Taken from Chen X et al; 2023.*

It has been reported that BAMBI is closely related to several pathologies such as inflammation, oxidative stress, adipogenesis, and cancer due the presence of variations in its expression levels in these pathologies (**Figure 7**) (Chen et al., 2023). For example, the expression of BAMBI is downregulated in the hepatocytes of mice with liver damage or liver fibrosis (Weber et al., 2023). In addition, in gastric cancer it has been described that BAMBI is abnormally expressed in gastric tissue, which could contribute to the upregulation of β-catenin signaling by inducing epithelial-mesenchymal transition and cell metastasis. Therefore, BAMBI could be a possible cause of the pathology and contributing to its aggressiveness (Liu et al., 2014).

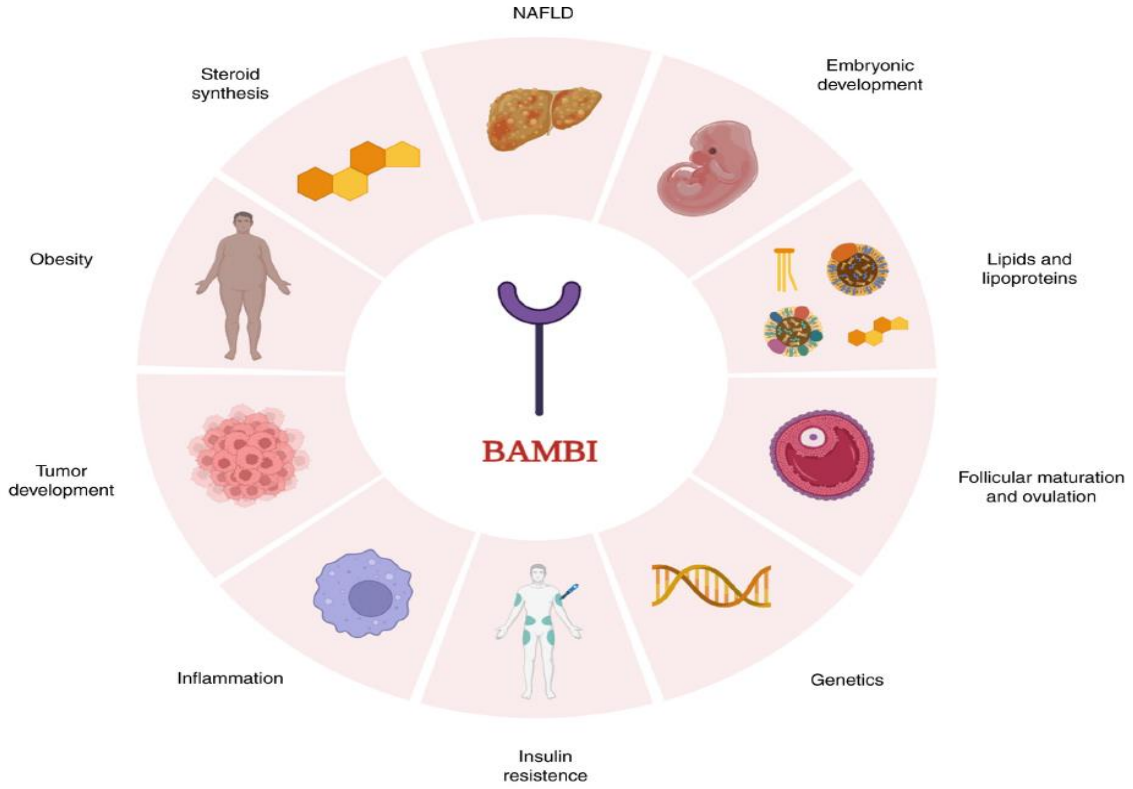

Figure 7. BAMBI and its role in several pathologies. **Taken from Chen X et al; 2023.*

BAMBI is capable to regulate CD25 expression and the intensity of IL-2 signaling in CD4+ T lymphocytes. For this reason, mice BAMBI$^{-/-}$ or treated with anti-BAMBI monoclonal antibody, show *in vivo* and *in vitro* increased and decreased in differentiation in Tregs and Th17, respectively (Postigo et al., 2016). This characteristic makes BAMBI a potential therapeutic target for the treatment of chronic inflammatory diseases. For example, in patients with obstructive pulmonary disease, it has been observed that following inflammation or exposure to cigarette smoke, BAMBI expression is upregulated by the activated immune system, which inhibits the generation of Tregs and induces a pathogenic T cell response where Th17 predominates in susceptible individuals (Zhang et al., 2016). On the other hand, BAMBI could promote the polarization process of anti-inflammatory M2 macrophages towards pro-inflammatory M1 macrophages blocking the signaling of TGF-β/Smad. The overexpression of BAMBI would decrease the ability of M2 macrophages to induce Tregs differentiation (S.-W. Sun et al., 2019).

BAMBI is a transmembrane protein with an inhibitory role in TGF-β-mediated signaling at the cell membrane level. Research carried out by our group has shown that the absence of BAMBI is associated with alterations in Treg cell populations *in vivo*, with an increase in the *in vitro* differentiation of Tregs from naïve CD4+ T lymphocytes. Tregs also have shown a potentiation in their suppressive activity, which protects against certain autoimmune diseases. This makes BAMBI a therapeutic target in chronic diseases. In addition, BAMBI deficiency in mice produces age-dependent thymic atrophy, manifesting as a smaller size and number of cells in this organ. With these outcomes, we propose the present work with the following objectives.

2. Objectives.

2.1. General objective.

To functionally characterize the different subpopulations of peripheral immune cells in BAMBI *knockout* mice.

2.2. Specific objectives.

1. To quantify the total number of splenic T cell and NK cell populations from BAMBI *knockout* (BAMBI-KO) and WT (wildtype) mice.
2. To identify T and NK cells subpopulations present in the spleens of BAMBI-KO and WT mice.
3. To study the differential susceptibility to spontaneous cell death of peripheral lymphocytes in presence versus absence of BAMBI.
4. To compare peripheral CD4+ and CD8+ T cell proliferation from BAMBI-KO and WT mice.
5. To evaluate if the absence of BAMBI modulates the activation and cytotoxic activity of NK cells.

3. Materials and methods.

3.1. Animals.

C57BL/6 (WT) mice were obtained from Charles River (Wilmington, Massachusetts; USA). The 129SvJ/B6 BAMBI-KO mice were generated as described by Tramullas and collaborators (Tramullas et al., 2010) and then crossed with C57BL/6 mice for up to twelve generations. Crossbreeding of BAMBI$^{+/-}$ mice resulted in homozygous mutants. The genotyping of these mice was confirmed by polymerase chain reaction (PCR) from genomic DNA that was extracted from blood samples from the tail. All live animal studies were approved by the Institutional Committee for the Care and Use of Laboratory Animals of the University of Cantabria and were carried out in accordance with the Declaration of Helsinki and the Directive of the Council of the European Communities (86/609/EEC).

3.2. Spleen extraction and sample preparation.

Mice have been euthanized to obtain their spleens, performing the procedure in the higher sterility possible. The spleens were placed in 50 mL falcon tubes with 10 mL of sterile phosphate buffered saline (PBS), keeping them on ice until processing. PBS was discarded from the tubes and the spleens were placed in petri dishes on 70 µm filters, then disaggregated using the plunger of a sterile syringe and washed with 2 mL of sterile PBS. The filtrate was transferred to new falcon tubes and centrifuged at 1500 rpm (revolutions per minute) for 5 minutes at 4°C. The supernatant was discarded, and the pellet was resuspended *with* 3 mL of red blood cell lysis buffer: 9 parts of lysis buffer II (0,89 g of NH4Cl in 100 mL of H2O) + 1 part of lysis buffer I (2,06 g of Tris in 100 mL of H20). 3 mL of lysis buffer per spleen was used. It was incubated for 5-7 minutes at room temperature. Finally, it was washed with 10 mL PBS, centrifuged at 1500 rpm for 5 minutes at 4°C and the supernatant was discarded. This last step was repeated once again, and then the cells obtained were resuspended in 10 mL of PBS. Cell counts were performed using *Countess 3* automated counter*,* Thermo Fisher Scientific (Waltham, Massachusetts; USA).

3.3. Characterization of Spleen T cell and NK cell populations.

T cell and NK cell populations were analyzed by flow cytometry using the *FACScanto* cytometer, Beckton-Dickinson (Franklin Lakes, New Jersey; USA). The analysis was performed from 2x10^6 spleen cells of BAMBI-KO and WT mice. Firstly, these cells were incubated for 10 minutes at room temperature with 30 µL of a 1:100 dilution of the supernatant of the IgG2b culture of anti-FcγRII rat (H2B4 hybridoma, clone 2.4G2) to block Fc receptors. Next, 50 µL from pools 1 and 2 were added to the corresponding tubes (**Table 1**). These pools are a mix of antibodies conjugated to different fluorophores:

FITC (fluorescein isothiocyanate), PE (phycoerythrin), PerCP (peridin-chlorophyll protein), APC (allophycocyanin), PerCP-Cγ5 (peridin-chlorophyll-cyanine-γ-5 protein), APC-Cγ7 (allophycocyanin-cyanine-γ-7) and PB (Pacific blue). Later, a 20-minute incubation at 4°C in the dark was carried out. Subsequently, the cells were washed twice with 2 mL of PBS, centrifuged at 1500 rpm for 5 minutes, and the supernatant was discarded. Finally, the cells were resuspended in 250 µL of PBS and kept at 4°C in the dark until the analysis in the flow cytometer. In the tubes with antibodies of the *pool* 1, before cell resuspension, 50 µL of *pool* 3 was added to the cells and incubated for 20 minutes at 4°C in darkness. It was then washed twice before resuspending the cells in 250 µL of PBS. The analysis of the results was carried out using the FACS Diva program, according to the expression profile of the markers.

Table 1. Antibodies used for the characterization of Spleen T and NK cell populations by flow cytometry.

Antibodies	Isotype	Clone	Fluorochrome	Pool
Murine anti-CD3ε	Hamster IgG1, κ.	145-2C11	FITC	1
Murine Anti-NK1.1	Rat IgG2a, κ.	PK136	Biotin	1
Murine Anti-CD49b	Rat IgM, κ.	DX5	PB	1
Murine Anti-CD27	Mouse IgG1, κ.	3D10	PE	1
Murine Anti-CD11b	Rat IgG2b, κ.	PK136	PerCP-Cγ5	1
Murine Anti-CD4	Rat IgG2b, κ.	GK1,5	PB	2
Murine Anti-CD8	Rat IgG2a, κ.	2.43	PerCP-Cγ5	2
Murine Anti-CD44	Rat IgG2b, κ	IM7	PE	2
Murine Anti-CD62L	Rat IgG2a, κ.	MEL-14	APC	2
Anti-B220 Murine	Rat IgG2a, κ.	RA3-6B2	FITC	2
Streptavidin			APC- Cγ7	3

3.4. Gating strategy

T lymphocytes, NK cells and their different populations present in the spleen were compared between WT and BAMBI-KO mice by flow cytometry. **Figure 8** shows the gating strategy used to analyze the different lymphocytes and NK cells subpopulations in this study. First, the area of the lymphocyte population (P1) was selected according to its size (FSC, Forward Scatter) and complexity (SSC, Side Scatter). In P1, possible doublets (aggregate of cells that could be detected in the flow cytometer as a single cell) were excluded according to their weight (FSC-H) and area (FSC-A) (P2). The B cells were then selected based on the expression of the B220 marker present in these cells. CD4+ and CD8+ T cells were selected from cells that did not express B220 marker, according to the expression of CD4 and CD8 molecules. The memory subpopulations of each group of lymphocytes were analyzed. Effector memory expressed the markers $CD62L^{-}CD44^{+}$; central memory $CD62L^{+}CD44^{+}$; and *naïve* T cells $CD62L^{+}CD44^{-}$ (**Figure 8.A**). The NK cells analysis was carried out from P2. Cells that did not express the CD3 marker in their membranes were selected. Subsequently, cells expressing CD49b and NK1.1 markers were selected for the analysis of the different subpopulations of NK cells. Immature NK cells have a $CD27^{+}CD11b^{-}$ phenotype; transitional cells $CD27^{+}CD11b^{+}$; and the mature NK cells $CD27^{-}CD11b^{+}$. Total NK cells are considered as the sum of NK cells with an $NK1.1^{+}CD49b^{+}$ and $NK1.1^{+}CD49b^{-}$ phenotype (**Figure 8.B**).

A

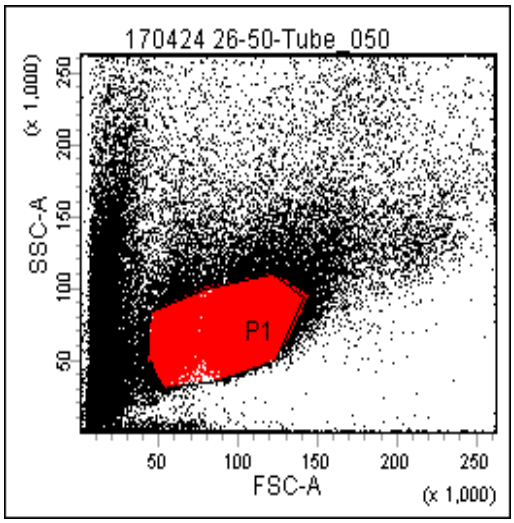
170424 26-50-Tube_050
SSC-A
(x 1,000)
P1
FSC-A
(x 1,000)

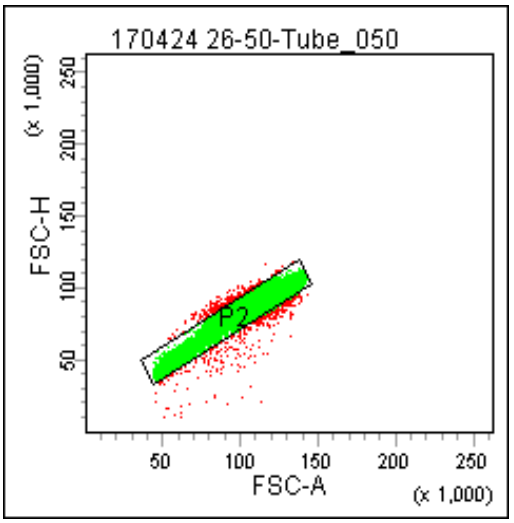
170424 26-50-Tube_050
FSC-H
(x 1,000)
P2
FSC-A
(x 1,000)

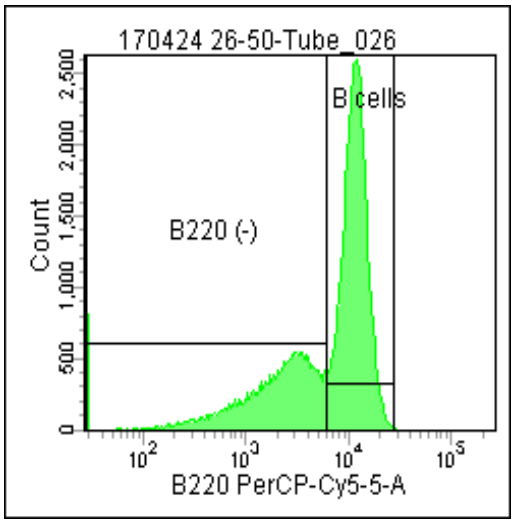
170424 26-50-Tube_026
Count
B cells
B220 (-)
B220 PerCP-Cy5-5-A

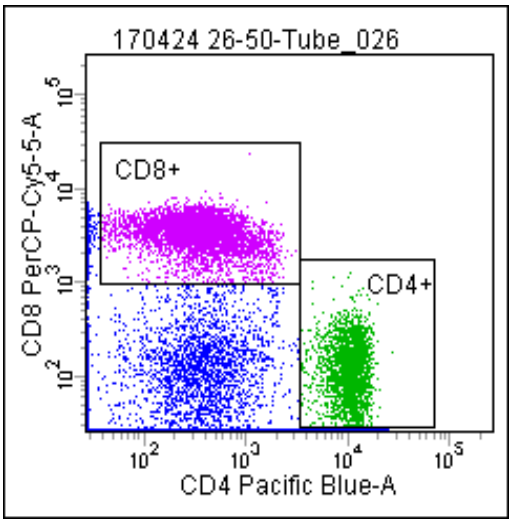
170424 26-50-Tube_026
CD8 PerCP-Cy5-5-A
CD8+
CD4+
CD4 Pacific Blue-A

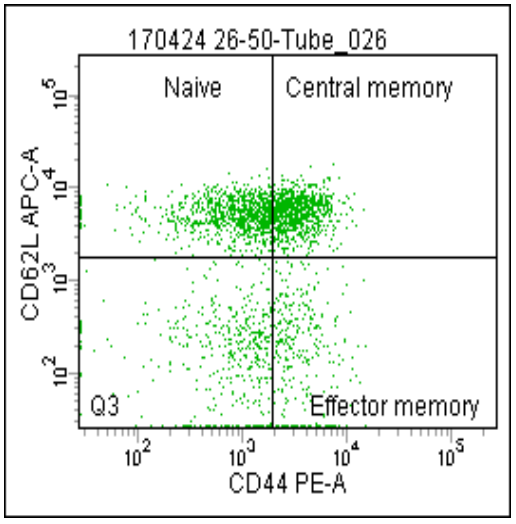
170424 26-50-Tube_026
Naive
Central memory
CD62L APC-A
Q3
Effector memory
CD44 PE-A

B

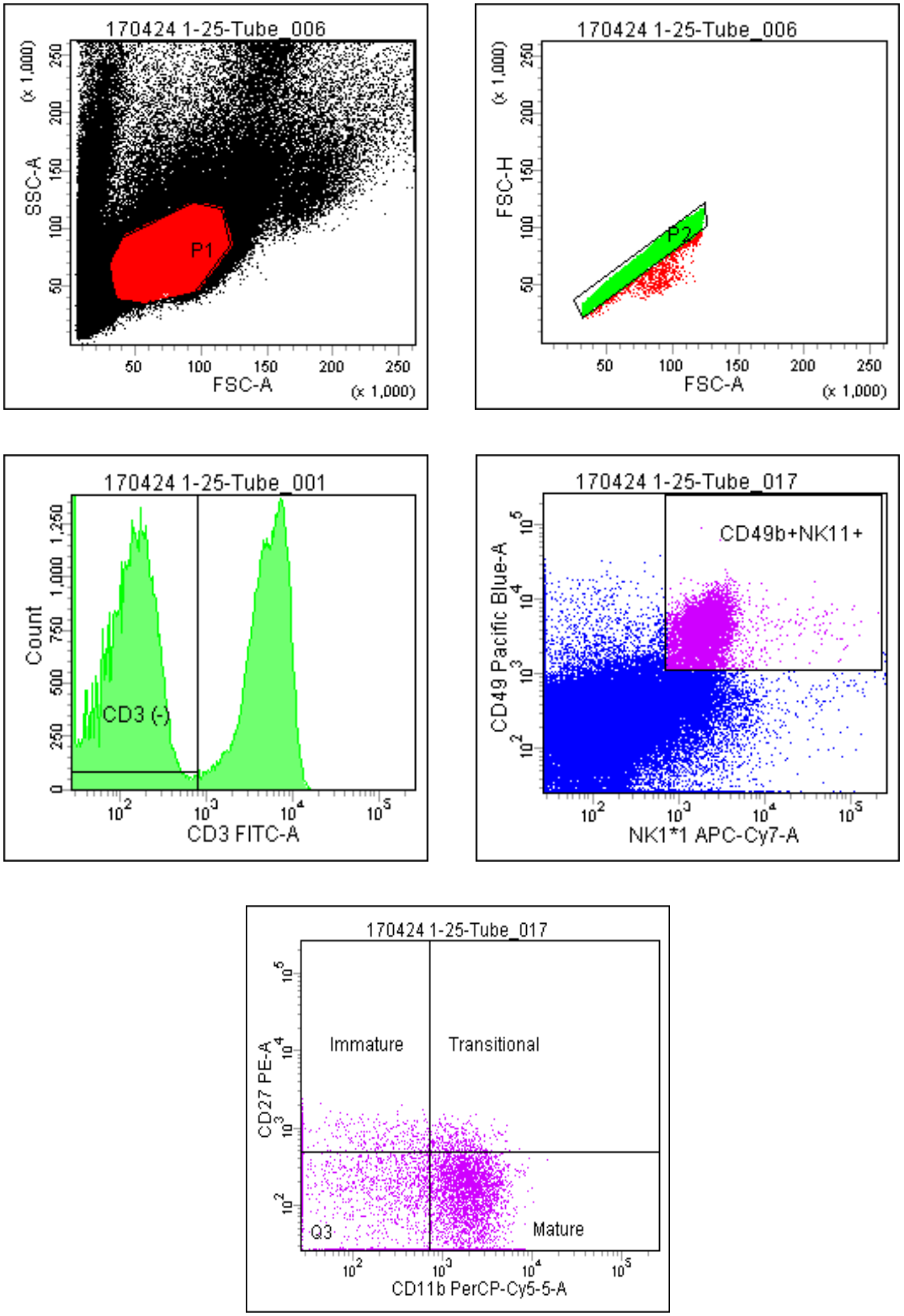

Figure 8. Gating strategy for the analysis of T and NK cells population of the spleen. Flow cytometry was performed on splenocytes from WT and BAMBI-KO mice. **A.** Gating strategy for the analysis of memory subpopulations of CD4+ and CD8+ T cells. **B.** Gating strategy for the analysis of subpopulations of NK cells.

3.5. CD4+ T cell purification.

The purification of CD4+ T cells has been performed using the *EasySePTM Mouse Naïve CD4+ T Cell Isolation kit,* StemCell Technologies (Vancouver, Canada) following the protocol provided by the manufacturer. A spleen cell concentration of 100x10^6 cells/mL was used with a volume range of 0,5-2 mL of sample. It was added 10 µL/mL of sample of *FcR blocker* and then the sample was transferred to a 5 mL polystyrene tube (12x75 mm). Next, it was added 50 µL/mL of sample of *Isolation cocktail*, mixed, and incubated at room temperature for 7,5 minutes. Afterward, 50 µL/mL of sample of *Depletion cocktail* was added, mixed, and incubated at room temperature for 2,5 minutes. Subsequently, 75 µL/mL of sample of *RapidSpheres™* was added, mixed, and incubated at room temperature for 2,5 minutes. Finally, PBS-FBS (98% PBS + 2% fetal bovine serum) was added up to a volume of 2,5 mL, lightly mixed and the tube without lid was placed inside a magnet, incubated for 10 minutes at room temperature, and later the supernatant was decanted (without removing the tube from the magnet) to a new 15 mL falcon tube. Cell counts were performed using the *Countess 3* automated counter, Thermo Fisher Scientific (Waltham, Massachusetts; USA). In addition, 1x10^5 cells were separated to verify their purification by flow cytometry.

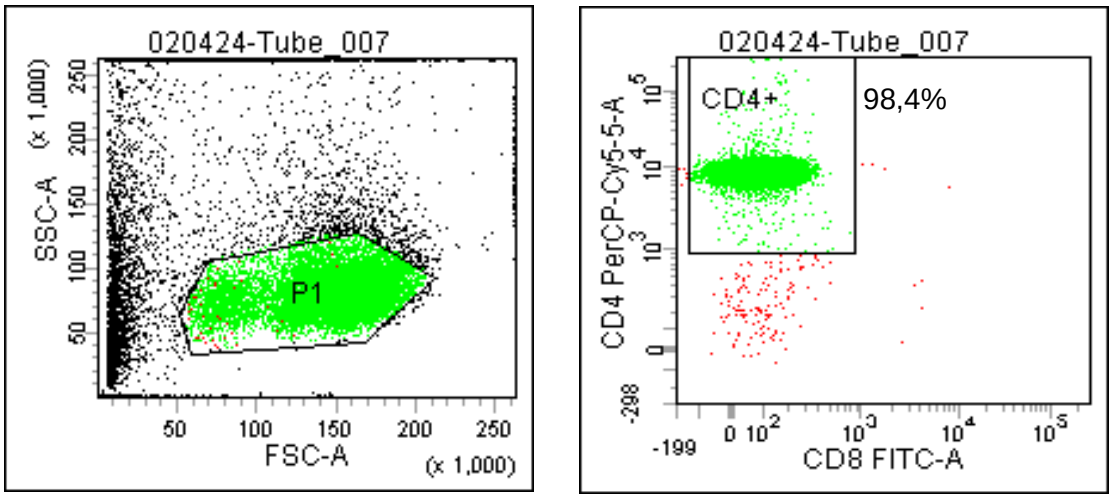

Figure 9. CD4+ T cells purification. The image shows the percentage of CD4+ T cells obtained after purification from mouse splenocytes.

3.6. CD8+ T cell purification.

The CD8+ T cells purification has been performed with the *EasySePTM Mouse CD8+ T Cell Isolation kit,* Stem Cell Technologies (Vancouver, Canada), according to the protocol provided by the manufacturer. Similarly, a splenocytes concentration of 100x10^6 cells/mL was used with a sample volume range of 0,5-2 mL. Firstly, 20 µL/mL of sample of *FcR blocker* was added and then the sample was transferred to a 5 mL polystyrene

tube (12x75 mm). Immediately, 50 µL/mL of sample of *Isolation cocktail* was added, mixed, and incubated at room temperature for 10 minutes. Later, 125 µL/mL of sample of *RapidSpheres*^{TM} was added, mixed, and incubated at room temperature for 5 minutes. Finally, PBS-FBS was added up to a volume of 2,5 mL, lightly mixed and the tube without lid was placed inside a magnet, incubated for 2,5 minutes at room temperature, and finally the supernatant was decanted (without removing the tube from the magnet) to a new 15 mL falcon tube. Cell counts were performed using the *Countess 3* automated counter, Thermo Fisher Scientific (Waltham, Massachusetts; USA). Also, 1x10^5 cells were separated to verify their purification by flow cytometry.

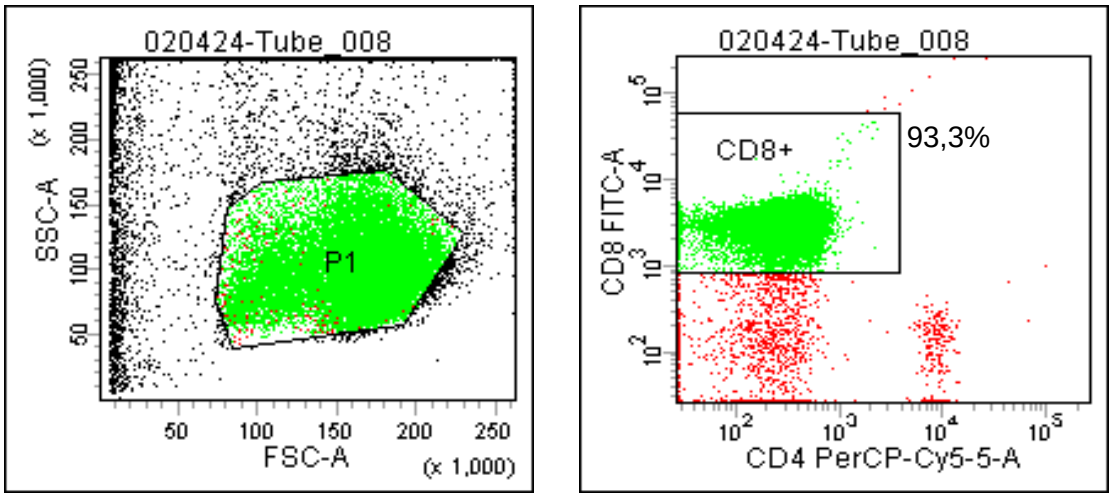

Figure 10. CD8+ T cells purification. The image shows the percentage of CD8+ T cells obtained after purification from mouse splenocytes.

3.7. Purification of NK cells.

The NK cells purification has been developed with the *EasySePTM Mouse NK Celll Isolation kit,* Stem Cell Technologies (Vancouver, Canada), according to the protocol provided by the manufacturer. A spleen cell concentration of 100x10^6 cells/mL was used with a volume range of 0,5-2 mL of sample. First, the sample was transferred to a 5 mL polystyrene tube (12x75 mm). Next, 50 µL/mL of sample of *Isolation cocktail* was added, mixed, and incubated at room temperature for 10 minutes. Subsequently, 100 µL/mL of sample of *RapidSpheres*^{TM} was added, mixed, and incubated at room temperature for 5 minutes. Finally, PBS-FBS was added up to a volume of 2,5 mL, lightly mixed, and the tube without lid was placed inside a magnet, incubated for 5 minutes at room temperature, and the supernatant was decanted (without removing the tube from the magnet) to a new 15 mL falcon tube. The last step was performed once again and then the two collected fractions were mixed in the same tube. Cell counts were performed using the *Countess 3* automated counter, Thermo Fisher Scientific (Waltham,

Massachusetts; USA). Similarly, 1x10^5 cells were separated to verify their purification by flow cytometry.

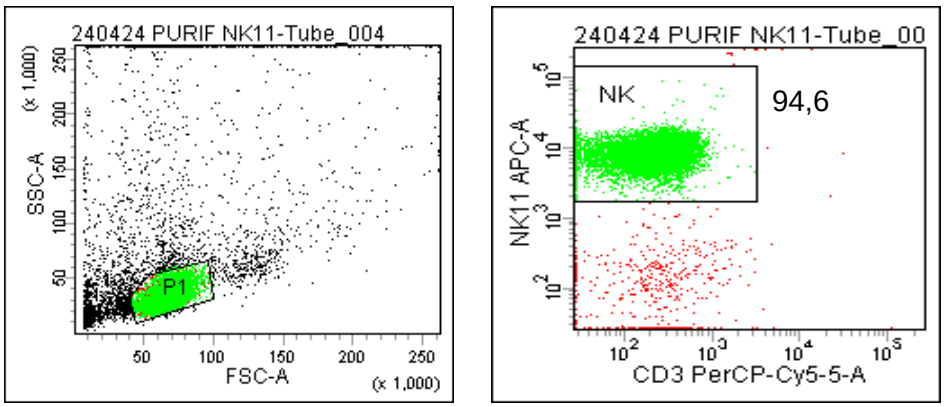

Figure 11. NK cells purification. The image shows the percentage of NK cells obtained after purification from mouse splenocytes.

3.8. Spontaneous cell death.

To assess spontaneous cell death of CD4+ and CD8+ T cells, it was first necessary to obtain and purify these cells from the spleens of WT and BAMBI-KO mice, as described above. After obtaining the purified cells, 1x10^5 cells per well were cultured in culture dishes with flat bottom in a final volume of 200 µL and incubated at 37°C for up to 72 hours. Culture has been performed using complete culture medium RPMI-1640, Sigma-Aldrich Corporation (St. Louis, Missouri; USA), supplemented only with 2-β-mercaptoethanol, without the addition of any stimulants such as antibodies or cytokines. Finally, the percentage of apoptotic cells was determined using trypan blue reagent after 24, 48 and 72 hours of culture, using the Neubauer chamber to count apoptotic and non-apoptotic cells.

3.9. CD4+ and CD8+ T cell proliferation assay.

The cell proliferation assay has been developed by labeling T cells with CFSE and subsequent culture in 96-well culture plates with a flat bottom. After purification of T cells, they were labeled with CFSE dye from the commercial *CellTraceTM Cell Proliferation kit,* Thermo Fisher Scientific (Waltham, Massachusetts; USA) following the manufacturer's instructions.

A cell concentration of 1x10^6 cells/mL (purified CD4+ and CD8+ T cells) was taken as a starting point since the protocol has been optimized for no more than this cell concentration. First, the *CellTraceTM CFSE* reagent was resuspended using 20 µL of dimethyl sulfoxide (DMSO). It is recommended that this reagent be resuspended only before use. Next, 1 µL of *CellTraceTM CFSE* was added for each 1 mL of cell suspension in PBS, mixed well, and incubated for 20 minutes at 37°C in darkness. Subsequently,

complete culture medium supplemented with 2-β-mercaptoethanol (RPMI-1640, Sigma-Aldrich Corporation (St. Louis, Missouri; USA)) was added up to 5 times the original volume, it was lightly mixed and re-incubated at 37°C for 5 minutes in darkness. Next, it was centrifuged at 1500 rpm for 5 minutes and the supernatant was discarded. The *pellet* was resuspended in 1 mL of preheated complete culture medium supplemented with anti-CD28 antibody at a concentration of 20 ng/mL.

Later, the cells were cultured in a 96-well culture dish with flat bottom that were previously coated with anti-CD3 antibody, using a solution with a concentration of 2,5 µg/mL of the antibody and incubated at 37°C for 1-3 hours. Were cultured $1x10^5$ CD4+ and CD8+ T cells (WT and BAMBI-KO) per well at 37°C in a final volume of 200 µL.

Finally, the proliferation of the different cell populations was analyzed using the flow cytometer *FACScanto*, Beckton-Dickinson (Franklin Lakes, New Jersey; USA). The analysis was performed after 72 hours of CD8+ cells culture, and 96 hours of CD4+ cells culture. The complete volume of the culture was collected from each well at the corresponding time and transferred to 5 mL polystyrene tubes for cytometry (12x75 mm). Two washes were performed with 2 mL of PBS, centrifuging at 1500 rpm for 5 minutes and discarding the supernatant. Finally, the cells were resuspended in 250 µL of PBS for analysis by the flow cytometer.

Were calculated proliferation, expansion, division, and replication index (**Table 2**) using FlowJo´s Proliferation tool, Beckton-Dickinson (Franklin Lakes, New Jersey; USA). This platform allows to calculate different divisions index in a proliferation assay that undergoes 3-6 divisions.

Table 2. Divisions index calculated with FlowJo´s platform.

Index	Formula
Division index	Total Number of Divisions/The number of cells at start of culture
Proliferation index	Total Number of Divisions/Cells that went into division
Expansion Index	Total Number of Cells/ The number of cells at start of culture
Replication Index	Total Number of Divided Cells/ Cells that went into division

3.10. *Ex vivo* cytotoxicity assay of murine NKs cells.

The NK cell-mediated cytotoxicity assay has been performed following the protocol provided by Wong and collaborators (Wong et al., 2021). Firstly, NK cells were activated *in vivo* 24 hours before the test in *2* BAMBI-KO mice and 2 WT mice after intraperitoneal

administration of 1,5 µg/µL of poly I:C. After 24 hours, the spleens of the mice were collected and the NKs cells were purified following the protocol described previously. Next, the NKs cells were cultured in 96-well V-bottom culture plates using complete culture medium supplemented with 10 ng/mL of IL-15 in a final volume of 100 µL per well. Culture was performed using different ratios of NKs cells per well: $2x10^5$ cells, $8x10^4$ cells, $4x10^4$ cells and $2x10^4$ cells. RMA-S cells (MHC-I deficient cells) were used as target cells, which were pre-labeled with CFSE, as described above in the proliferation assay. Immediately, they were added to the culture plate in the corresponding wells in an amount of $4x10^4$ cells per well using complete culture medium supplemented with 10 ng/mL of IL-15 in a final volume of 100 µL per well. In addition, control wells were added, consisting of single target cells, unlabeled target cells, 7-AAD-labeled target cells alone, and CFSE-labeled target cells, all of them at a rate of $4x10^4$ cells per well with a final volume of 200 µL of complete medium supplemented with 10 ng/mL of IL-15 (**Figure 12**). 5 µL of 7-AAD was added 5 minutes *prior* to analysis of each well by the flow cytometer.

For each ratio of NK cells:target cells, the percentage of specific death was calculated as:

$$[\%7\text{-AAD+ of CFSE+ cells}]_{(\text{NKs + target cells})} - [\%7\text{-AAD+ of CFSE+ cells}]_{(\text{single target cells})}$$

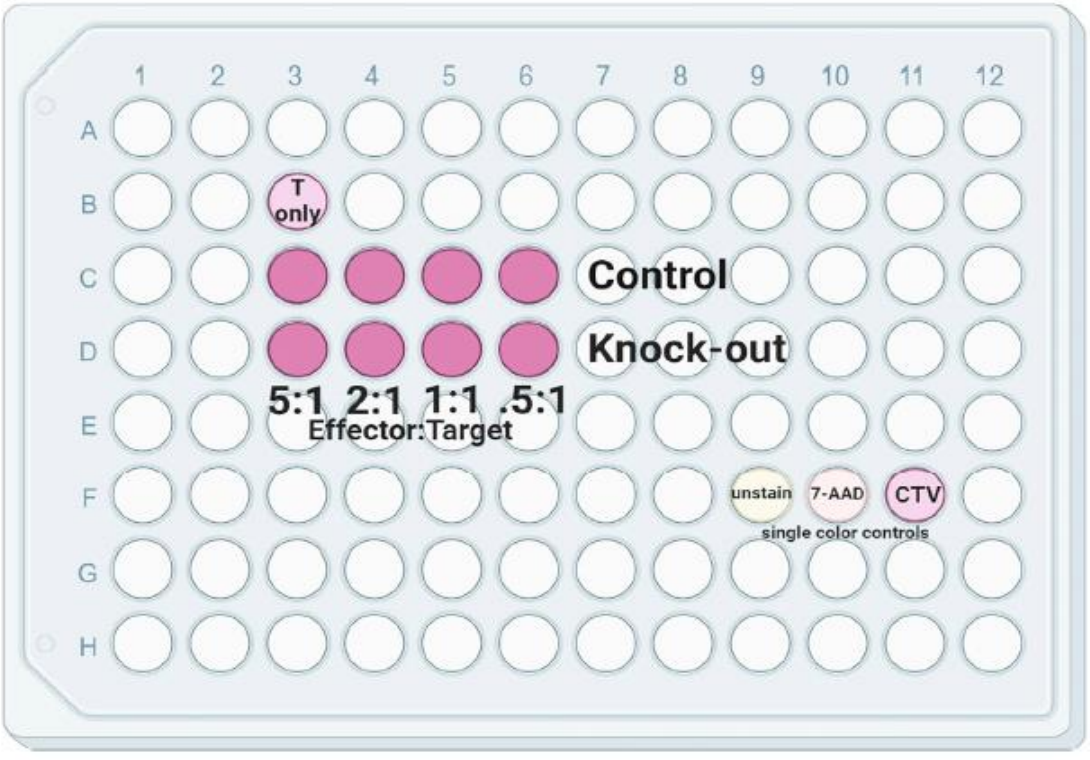

Figure 12. Example of NK cell-mediated cytotoxicity assay. **Taken from Wong et al; 2021.*

3.11. Assessment of NK cells activation trough Granzyme B expression.

To evaluate the activation of NK cells after intraperitoneal administration of poly I:C to WT and BAMBI-KO mice, Granzyme B was labeled to evaluate its expression. Whole blood samples were taken from WT and BAMBI-KO mice *prior* to administration of poly I:C for use as controls. After 24 hours of administration of poly I:C and purification of NK cells from the spleens of WT and BAMBI-KO mice, $1x10^6$ of these cells were separated from each group for labeling. First, the cells were incubated for 10 minutes at room temperature with 30 µL of a 1:100 dilution of the supernatant of the anti-FcγRII rat IgG2b culture (H2B4 hybridoma, clone 2.4G2) to block Fc receptors. Next, 50 µL of the "*Surface staining*" pool (**Table 2.3**) was added to the corresponding tubes and incubated for 20 minutes at 4°C in the dark. Subsequently, the cells were washed twice with 2 mL of PBS, centrifuged at 1500 rpm for 5 minutes, discarding the supernatants. Then, the process of fixation and permeabilization of the cells was carried out using 200 µL of a fixation/permeabilization solution [mix of diluent and concentrate] (Fixation/Permeabilization diluent and concentrate**,** *eBioscience*) in a 3:1 ratio, incubated for 30 minutes at 4°C in the dark. After washing with 10X Permeabilization Buffer (*eBioscience*; diluted to 1X in H2O(d)), the cell suspensions were incubated for 40 minutes at 4°C in the dark with 50 uL of the "*Granzyme B*" pool (**Table 3**) for intracellular labeling. Finally, the cells were washed again twice with 2 mL PBS and finally resuspended in 250 µL PBS to be analyzed in the *FACScanto* flow cytometer, Beckton-Dickinson (Franklin Lakes, New Jersey; USA).

Table 3. Antibodies used to assess the expression of Granzyme B in NK cells.

Antibodies	Isotype	Clone	Fluorochrome	Pool
Murine anti-CD3ε	Hamster IgG1, κ.	145-2C11	PerCP-Cγ5	*Surface staining*
Murine Anti-NK1.1	Rat IgG2a, κ.	PK136	APC	*Surface staining*
Murine Anti-CD49b	Rat IgM, κ.	DX5	PB	*Surface staining*
Murine Anti-Granzyme B	Mouse IgG1, κ.	QA16A02	FITC	*Granzyme B*

3.12. Statistical analysis.

To compare number and percentage of cells obtained from the experimental and control group has been used a non-parametric test, the Mann Whitney test. Instead, it has been used Two Way RM-ANOVA test to compare outcomes obtained in the spontaneous cell death, proliferation and cytotoxicity assay. Significant differences were considered as no significant $p \geq 0,05$ (ns); significant $p < 0,05$ (*); very significant $p < 0,01$ (**); strongly significant $p < 0,001$ (***); and highly significant $p < 0,0001$ (****). Graphics and statistical analysis have been made using the software *GraphPad Prism* version *8.0*.

4. Results

4.1. Phenotypic characterization of lymphocyte and NK cell populations in the spleen of BAMBI-KO mice.

The phenotypic characterization of the different lymphocyte populations including T cells and NK cells from the spleen of WT and BAMBI-KO at different ages were performed by flow cytometry. Previously, the number of splenocytes were determined by cell counter. According to our results, BAMBI-KO mice showed no significant differences compared to WT mice at all ages (**Figure 13**).

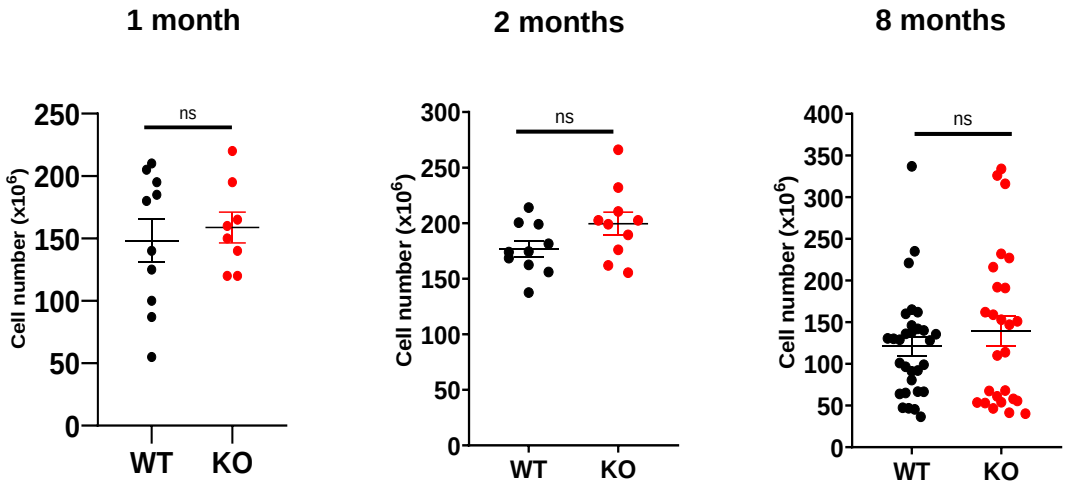

Figure 13. Total number of cells from the spleen of WT (black) and BAMBI-KO (red) mice at 1, 2, and 8 months old. Each symbol represents an individual mouse. Mean is displayed ± Standard Error of the Mean (SEM). Data were compared using Mann Whitney test. ns (p≥0,05); * (p<0,05); ** (p<0,01); *** (p<0,001); **** (p<0,0001).

Using flow cytometry, the quantification of the number of the different subtypes of lymphocytes populations in the spleen showed no significant changes in both CD4+ and CD8+ T cells in BAMBI-KO respect to BAMBI-WT mice (**Figure 14.A&B**). These data do not correlate with our previous result showing a greater thymic involution in absence of BAMBI. In contrast, NK cells showed a significant increase in the number of cells in the BAMBI-KO group compared to BAMBI-WT individuals in 1- and 2-month-old mice (**Figure 14.C**). Similarly to T cells, B cells showed no significant alterations in the number of cells when BAMBI-KO mice and BAMBI-WT mice were compared at 1- and 8-months age (**Figure 14.D**).

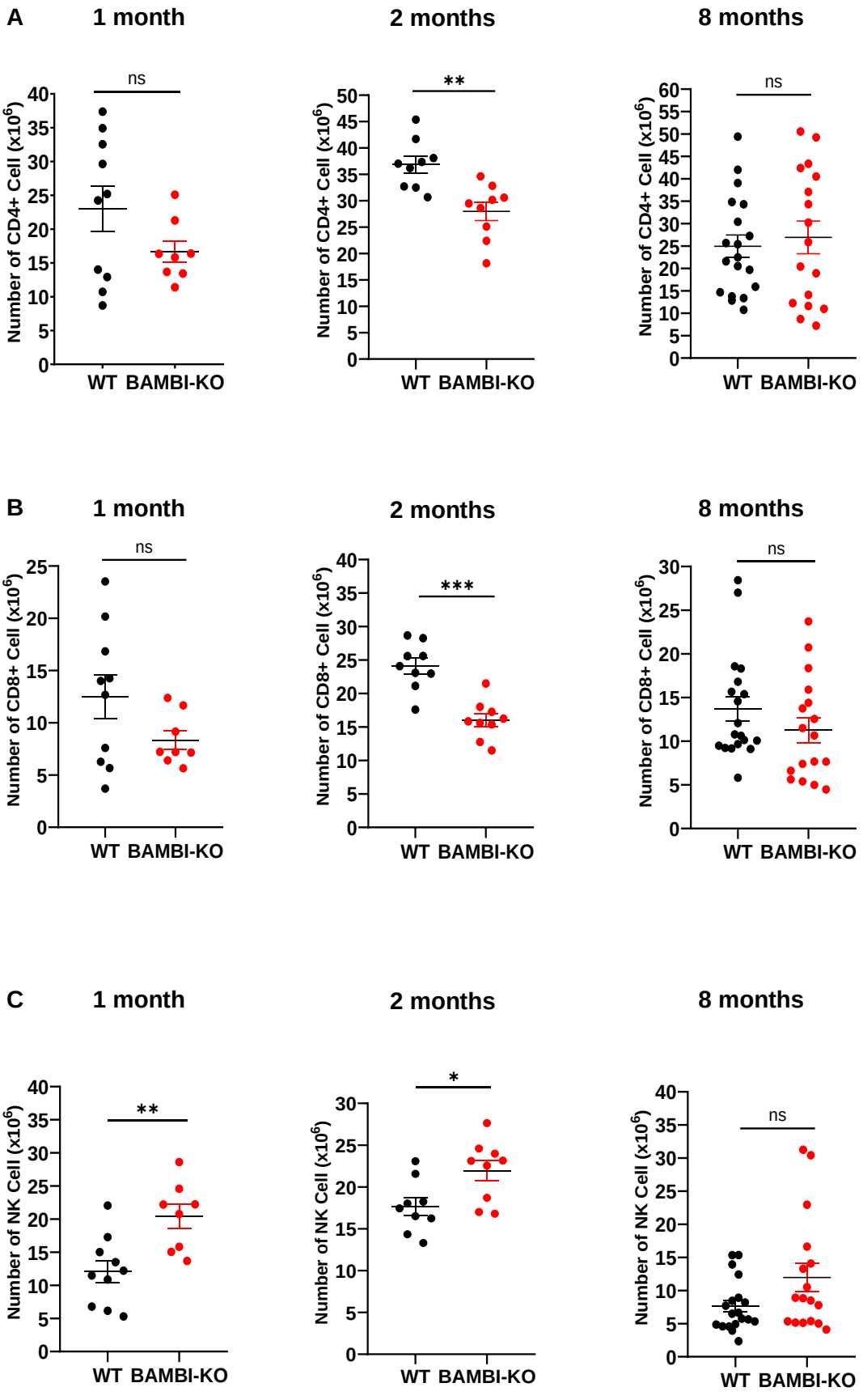
A
1 month
2 months
8 months
ns
**
ns
Number of CD4+ Cell (x10^6)
WT BAMBI-KO
B
1 month
2 months
8 months
ns
***
ns
Number of CD8+ Cell (x10^6)
WT BAMBI-KO
C
1 month
2 months
8 months
**
*
ns
Number of NK Cell (x10^6)
WT BAMBI-KO

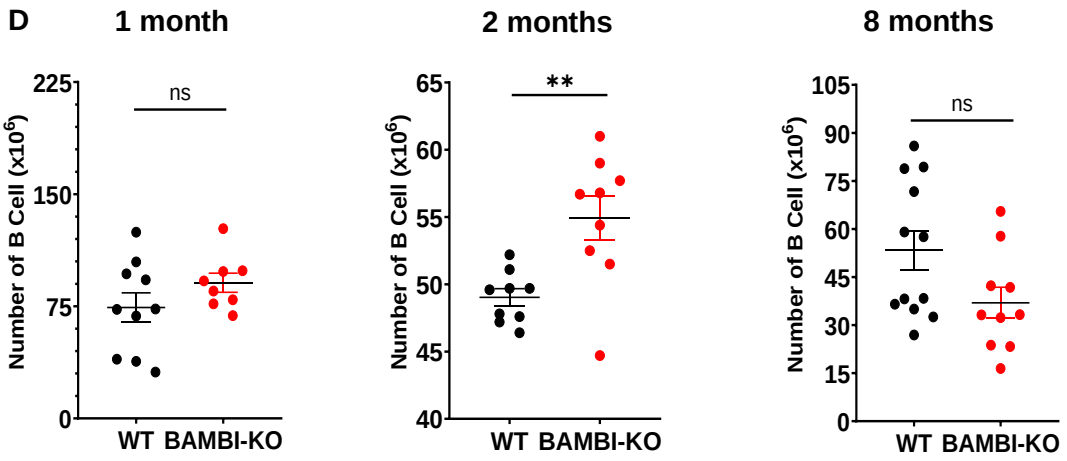

Figure 14. Total number of T cell populations and NK cells from the spleen of WT (black) and BAMBI-KO mice (red). A. Total number of CD4+ T cells from the mouse spleen. **B.** Total number of CD8+ T cells from the mouse spleen. **C.** Total number of NK cells from the mouse spleen. **D.** Total number of B cells from the mouse spleen. Calculating by extrapolating the percentage of each population to the total number of spleen cells in the organ. Each symbol represents an individual mouse. Mean is displayed ± SEM. Data were compared using Mann Whitney test. ns (p≥0,05); * (p<0,05); ** (p<0,01); *** (p<0,001); **** (p<0,0001).

Next, in order to study the functionality state of CD4+ and CD8+ T cells, we determined their naïve, central and effector memory subpopulations. BAMBI-KO mice showed an increase in the percentage of CD4+ effector memory T cells compared to WT group at all evaluated ages (**Figure 15.A**). Interestingly, these alterations correlate with the decrease of *naïve* CD4+ T cells (**Figure 15.B**). Increased central memory CD4+ T cells are also observed in 8-month-old mice (**Figure 15.C**). The same scenario was presented by the CD8+ memory T cell subpopulations where there was an increase in the percentage of effector and central memory cells in the BAMBI-KO group of mice compared to WT group (**Figure 16.A&C, respectively**) and a decrease in *naïve* cells whereas these alterations are not observed in younger mice (**Figure 16.B**). In addition, NK cells showed an increase in the percentage of the mature subpopulation in the BAMBI-KO mouse group compared to the WT group in 2- and 8-month-old mice (**Figure 17.A**) that correlates with decreased number of immature NK cells. At 1- and 2-month mice already showed lower immature and transition NK cells (**Figure 17.B&C**).

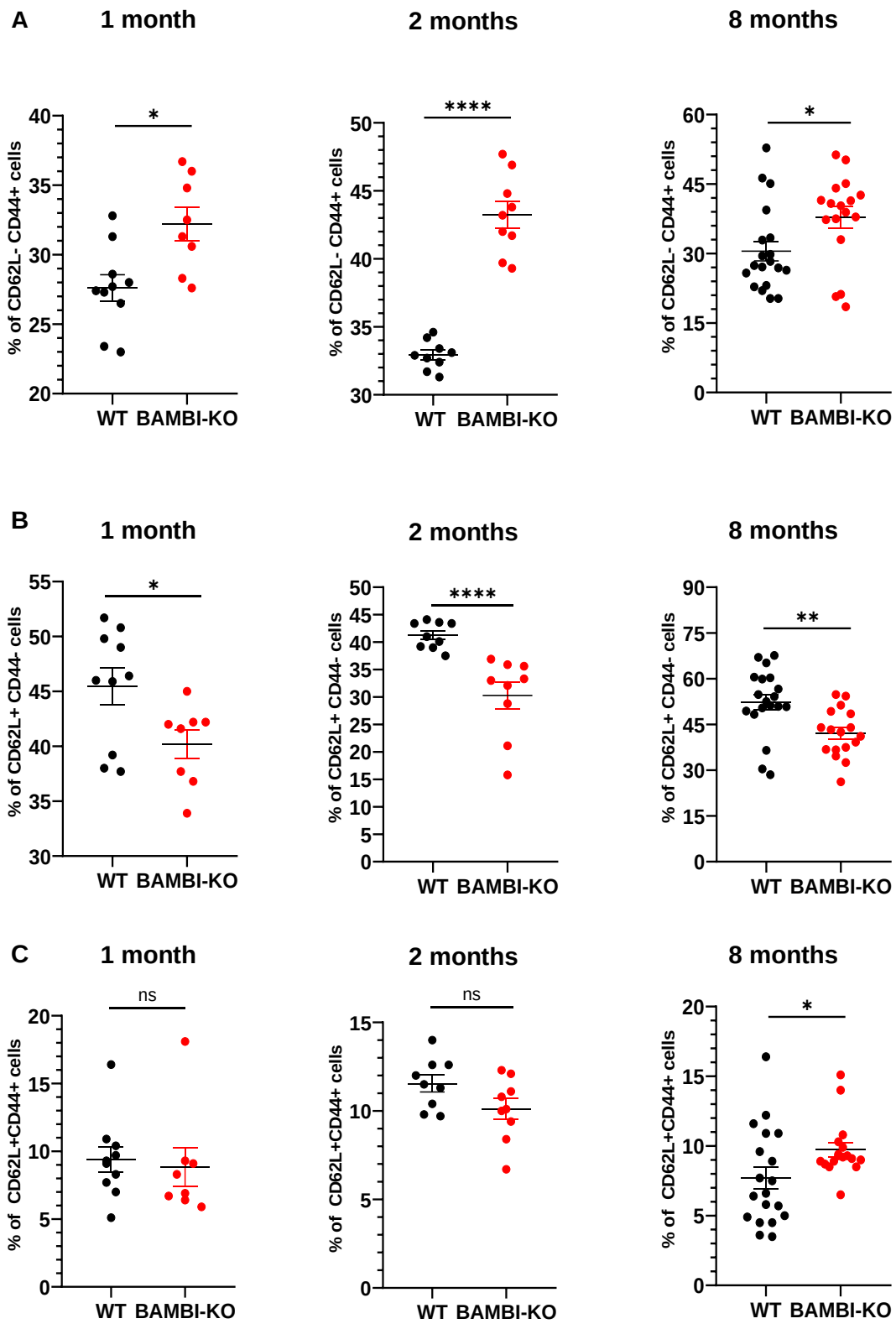

Figure 15. Percentage of T CD4+ memory cells subpopulation in the spleen of WT (black) and BAMBI-KO (red) mice. A. Percentage of CD4+ effector memory T cells in the spleen of WT (black) and BAMBI-KO (red) mice. **B.** Percentage of CD4+ *naïve* T cells in the spleen of WT (black) and BAMBI-KO (red) mice. **C.** Percentage of CD4+ central memory T cells in the spleen of WT (black) and BAMBI-KO (red) mice. Each symbol represents an individual mouse. Mean is displayed ± SEM. Data were compared using Mann Whitney test. ns (p≥0,05); * (p<0,05); ** (p<0,01); *** (p<0,001); **** (p<0,0001).

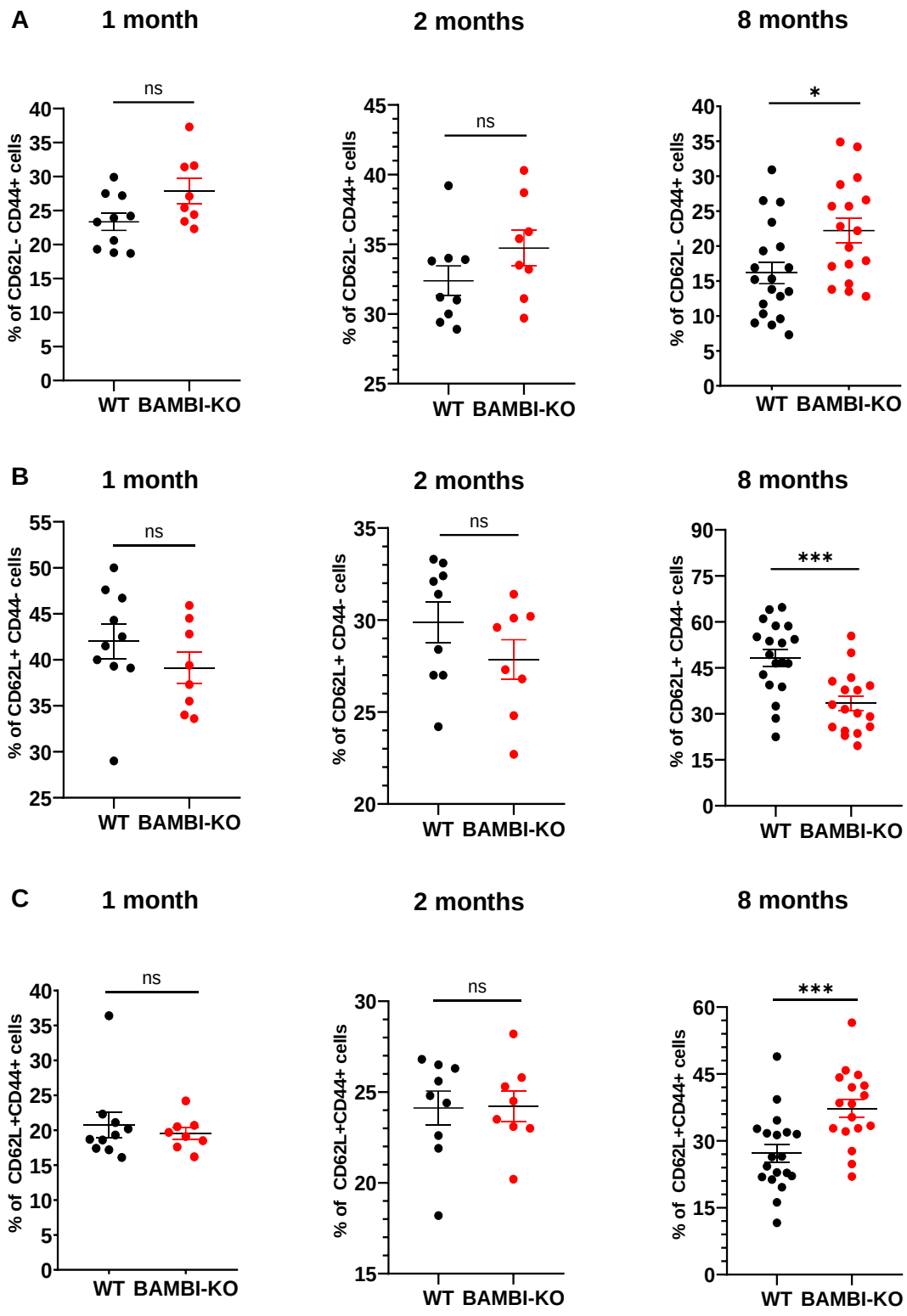

Figure 16. Percentage of T CD8+ memory cells subpopulation in the spleen of WT (black) and BAMBI-KO (red) mice. A. Percentage of CD8+ effector memory T cells in the spleen of WT (black) and BAMBI-KO (red) mice. **B.** Percentage of CD8+ *naïve* T cells in the spleen of WT (black) and BAMBI-KO (red) mice. **C.** Percentage of CD8+ central memory T cells in the spleen of WT (black) and BAMBI-KO (red) mice. Each symbol represents an individual mouse. Mean is displayed ± SEM. Data were compared using Mann Whitney test. ns (p≥0,05); * (p<0,05); ** (p<0,01); *** (p<0,001); **** (p<0,0001).

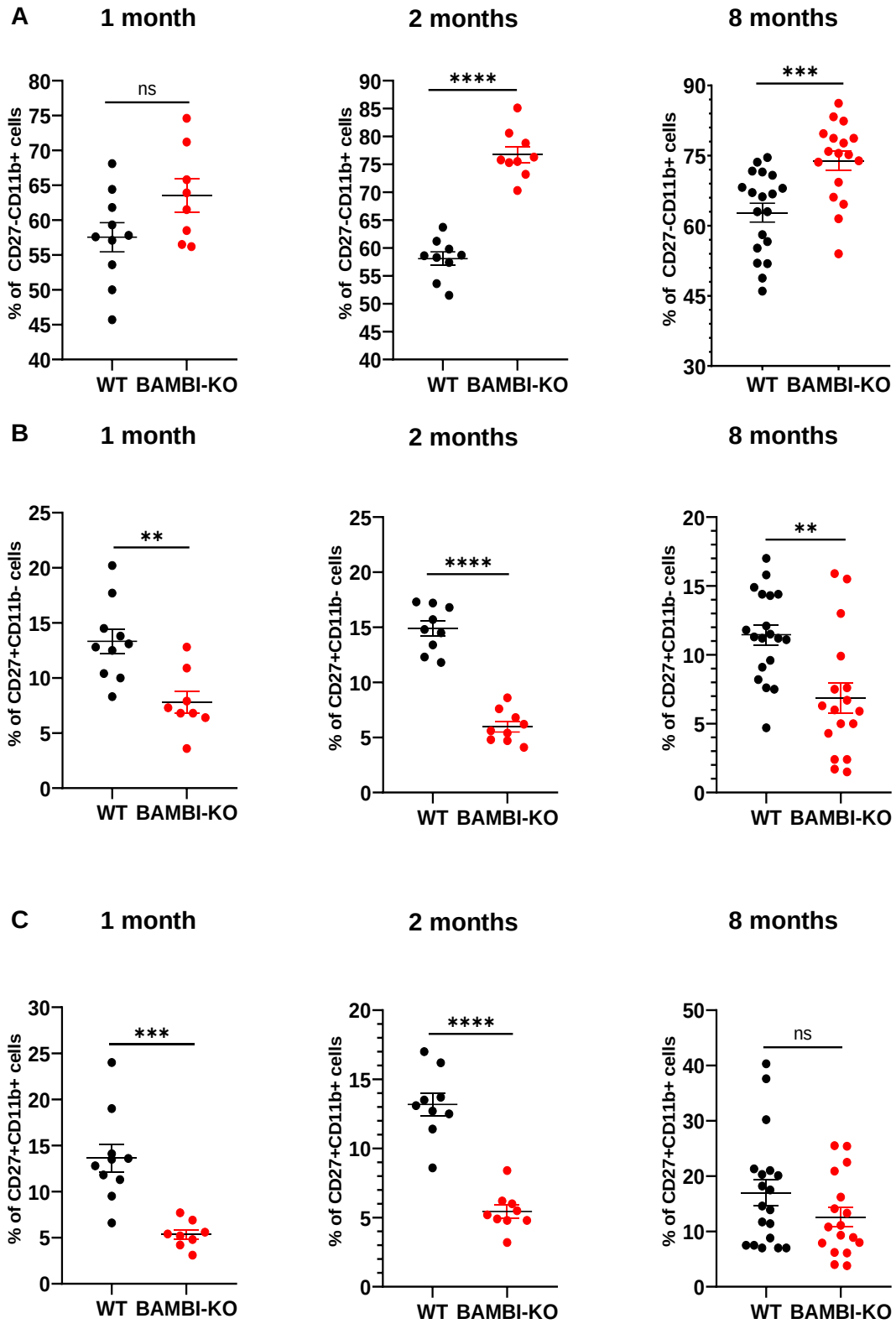

Figure 17. Percentage of NK cells subpopulation in the spleen of WT (black) and BAMBI-KO (red) mice. A. Percentage of mature NK cells in the spleen of WT (black) and BAMBI-KO (red) mice. **B.** Percentage of immature NK cells in the spleen of WT (black) and BAMBI-KO (red) mice. **C.** Percentage of transitional NK cells in the spleen of WT (black) and BAMBI-KO (red) mice. Each symbol represents an individual mouse. Mean is displayed ± SEM. Data were compared using Mann Whitney test. ns (p≥0,05); * (p<0,05); ** (p<0,01); *** (p<0,001); **** (p<0,0001).

4.2. Effect of BAMBI on spontaneous cell death of peripheral T lymphocytes.

Since spontaneous cell death is a parameter used to determine the maintenance of cell homeostasis, especially immune cells, the viability of peripheral CD4+ and CD8+ T cells has been determined. CD4+ and CD8+ T cells obtained from the spleens of BAMBI-WT and BAMBI-KO mice were cultured in the absence of any stimulus. The analysis was performed after 24, 48, and 72 hours of culture. The blue trypan reagent was used to count apoptotic cells using the Neubauer chamber. The percentage of viable cells was determined from the total number cells. Both groups of mice, BAMBI- WT and BAMBI-KO, did not show significant differences in the percentage of viability of CD4+ and CD8+ T cells at different times (**Figure 18**).

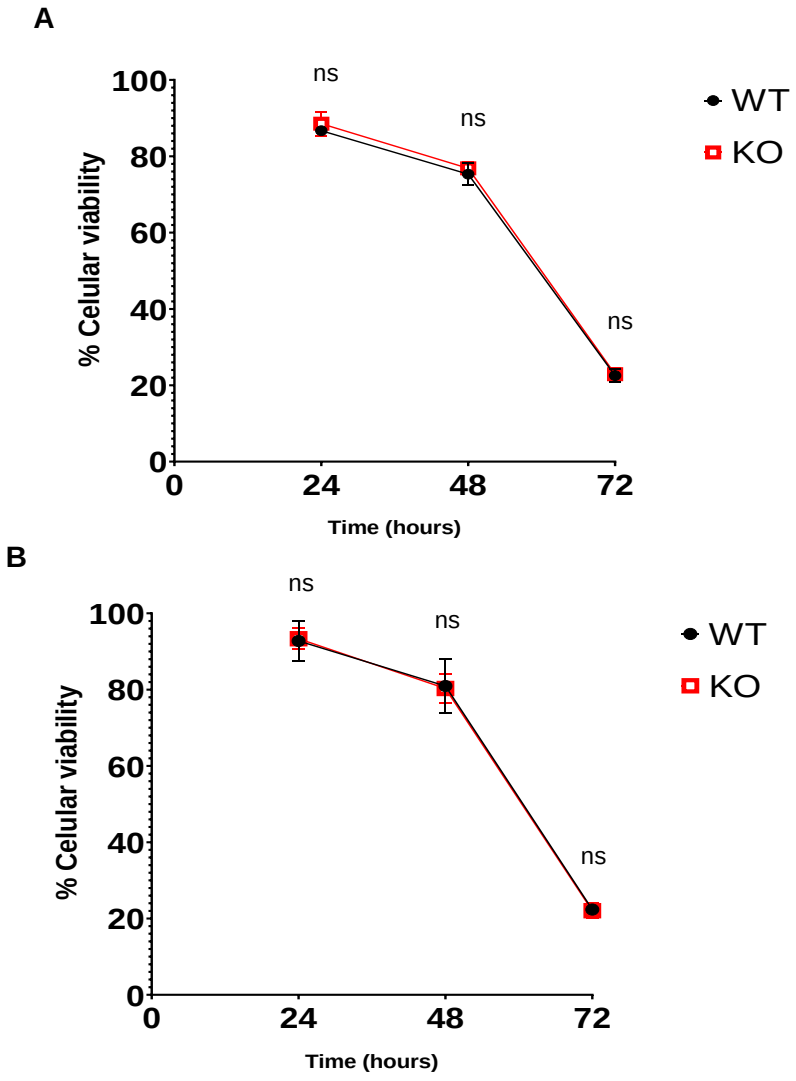

Figure 18. Percentage of cell viability at different times of CD4+ and CD8+ T cells from the spleen cells of WT (black) and BAMBI-KO (red) mice. A. Percentage of cell viability of WT and BAMBI-KO CD4+ T cells. **B.** Percentage of cell viability of WT and BAMBI-KO CD8+ T cells. Mean from duplicated experiments is displayed ± Standard Deviation (SD). Data were compared using Two Way RM-ANOVA test. ns (p≥0,05); * (p<0,05); ** (p<0,01); *** (p<0,001); **** (p<0,0001).

4.3. The lack of BAMBI expression increases cell proliferation of peripheral CD4+ and CD8+ T lymphocytes.

Owing to that rapid growth and proliferation of activated T cells are important features of an appropriate immune response, we have proposed to analyze the proliferative ability of CD4+ and CD8+ T lymphocytes. CD4+ and CD8+ T cells from BAMBI-KO and BAMBI-WT mice were used to perform a proliferation assay in response to anti-CD3 and anti-CD28 antibodies. CD8+ and CD4+ T cells were labeled with CFSE, stimulated for 72 hours and 96 hours respectively, and subsequently analyzed by the flow cytometer to evaluate the rates of division of these cells. CD4+ T cells from BAMBI-KO mice showed increased proliferation at 96 hours with a proliferation index of 1,56 (±0,08); while WT group showed a proliferation index of 1,2 (±0,17) (**Figure 19**). CD8+ T cells from BAMBI-KO mice also showed greater proliferation at 72 hours compared to the WT group, with a proliferation index of 1,78 (±0,17) for the BAMBI-KO group and 1,41(±0,33) for the WT group (**Figure 20**).

A

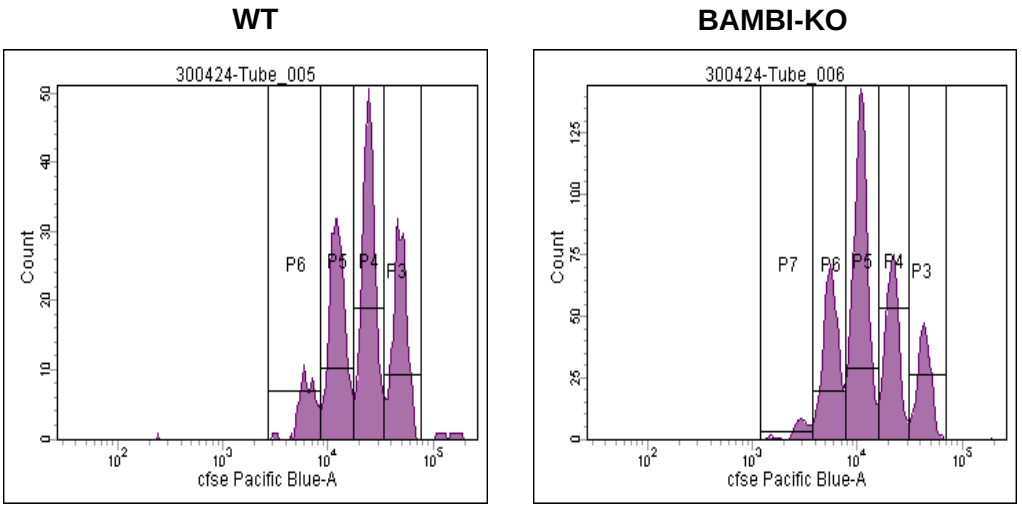

B

Index	WT	BAMBI-KO
Division index	0,45 (±0,29)	0,96 (±0,07)
Proliferation index	1,2 (±0,17)	1,56 (±0,08)
Expansion index	1,56 (±0,41)	2,44 (±0,16)
Replication index	2,43 (±0,39)	3,34 (±0,21)

Figure 19. Proliferation assay of CD4+ T cells with anti-CD3 and anti-CD28 antibodies stimulation. A. WT and BAMBI-KO CD4+ T cells division analyzed by FACS analysis. **B.** Division index of WT and BAMBI-KO CD4+ T cells obtained from the analysis with FlowJo´s platform. Mean from duplicated experiments is displayed ± SD.

A

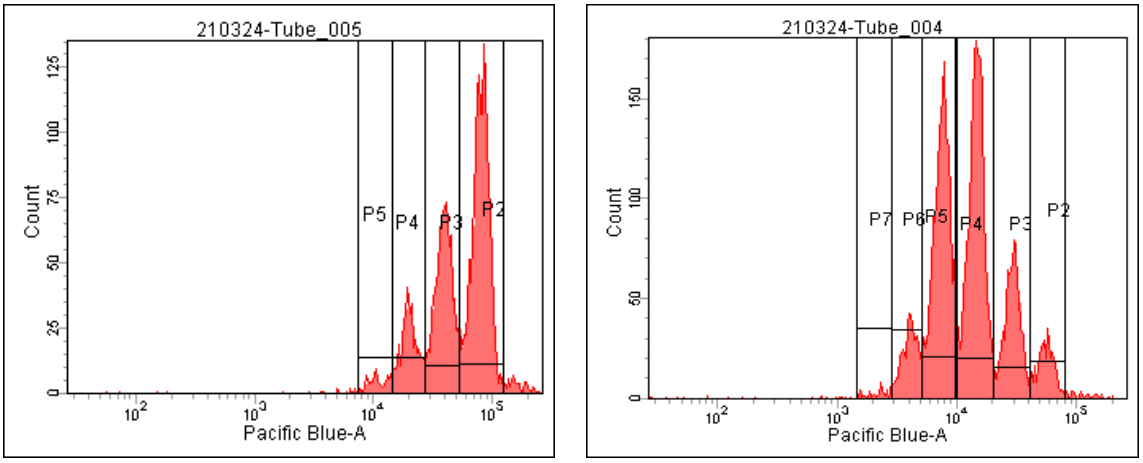

B

Index	WT	BAMBI-KO
Division index	0,59 (±0,43)	1,17 (±0,42)
Proliferation index	1,41 (±0,33)	1,78 (±0,17)
Expansion index	1,91 (±0,18)	3,08 (±0,8)
Replication index	3,04 (±0,95)	4,15 (±0,41)

Figure 20. Proliferation assay of CD8+ T cells with anti-CD3 and anti-CD28 antibodies stimulation. A. WT and BAMBI-KO CD8+ T cells division analyzed by FACS analysis. **B.** Division index of WT and BAMBI-KO C8+ T cells obtained from the analysis with FlowJo´s platform. Mean from duplicated experiments is displayed ± SD.

These results show that the reduction of thymocytes in BAMBI-KO is compensated peripherally by higher T cell proliferation.

4.4. The absence of BAMBI causes an increase in NK cell-mediated cytotoxicity.

BAMBI is a protein that plays an important role in the regulation of immune responses, mainly in inflammation, antitumor and autoimmune response. For this reason, its role in the missing-self recognition has been studied by measuring the cytotoxicity mediated by NK cells against RMA-S cells. To evaluate the cytotoxic capacity of BAMBI-KO versus BAMBI-WT NK cells, 24 hours before NK were isolated, they were activated *in vivo* upon intraperitoneal administration of poly I:C. Subsequently, the isolated NK cells were incubated at different ratios with RMA-S cells (target cells), which

were labeled with CFSE. After incubation, 7-AAD was added to the cell mixture to determine which CFSE labeled cells were lysed.

NKs cells from BAMBI-KO mice had a higher cytotoxic capacity compared to BAMBI-WT cells, due to the higher percentage of lysis in all the ratios used (**Figure 21**).

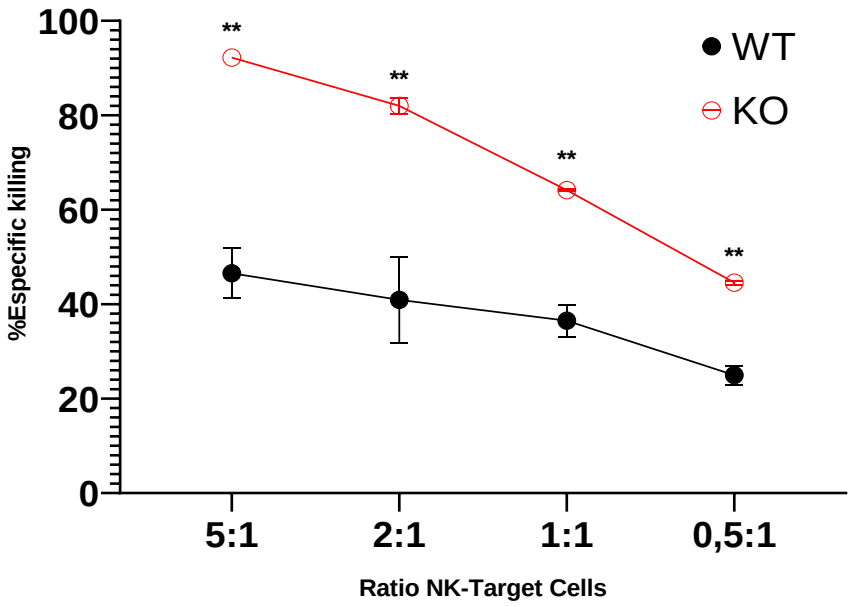

Figure 21. ***Ex vivo*** **cytotoxicity assay of NK cells from the spleen of WT (black) and BAMBI-KO (red) mice.** Mean from duplicated wells is displayed ± SD. Data were compared using Two Way RM-ANOVA test. ns (p≥0,05); * (p<0,05); ** (p<0,01); *** (p<0,001); **** (p<0,0001).

Cytotoxic activity in activated NK cells is mediated by Granzyme B which is secreted along perforin to mediate the apoptosis of target cells. To confirm our cytotoxicity results, the levels of Granzyme B in the BAMBI-WT and BAMBI-KO NK cells were analyzed by flow cytometry. The outcomes showed in **Figure 22** indicate a higher expression of Granzyme B in BAMBI-KO NKs cells with a mean fluorescence intensity (MFI) of 4342 compared to BAMBI-WT cells (MFI:1373). Therefore, the observed higher cytotoxicity present in BAMBI-KO NK cells is due to the successful mobilization of cytotoxic granules.

A **WT** **BAMBI-KO**

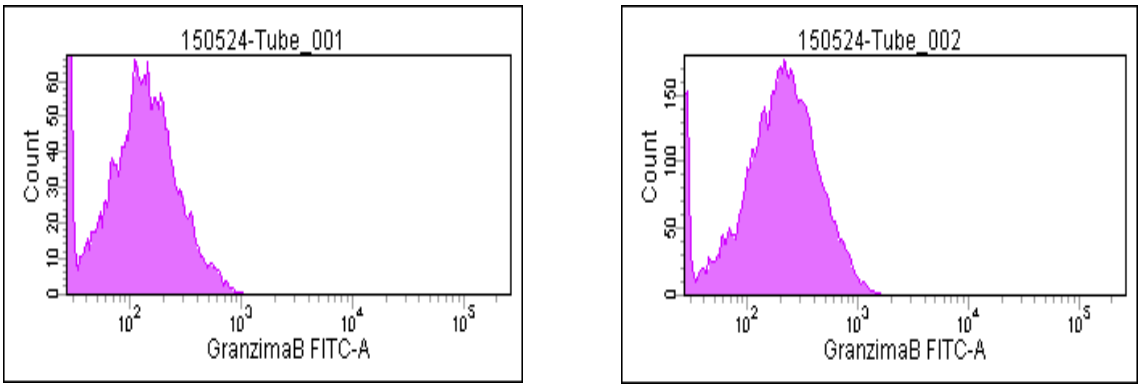

B

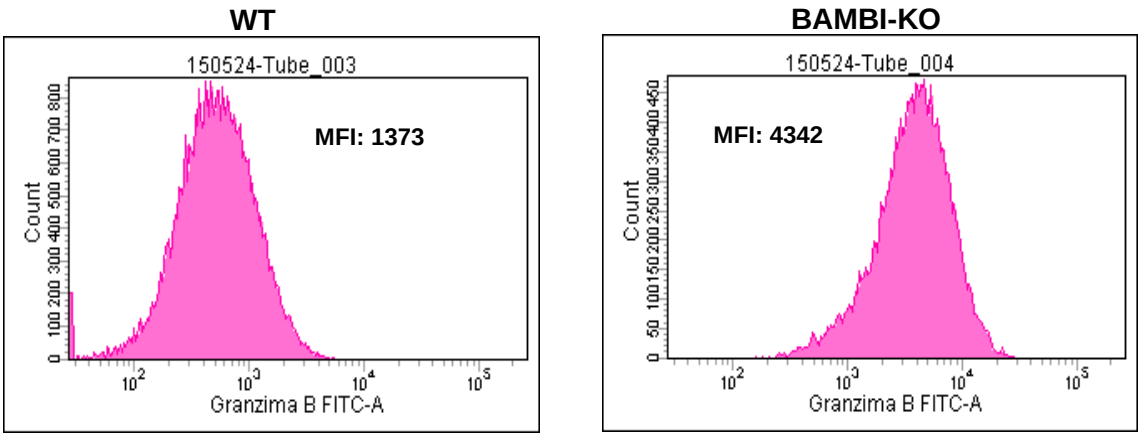

Figure 22. Granzyme B expression levels in NK cells from the spleen of WT and BAMBI-KO mice. A. Expression of Granzyme B in NK cells *prior* Poly I:C administration. **B.** Expression of Granzyme B in NK cells after Poly I:C administration.

5. Discussion

TGF-β is a potent regulatory cytokine with an important role in maintaining tolerance via regulation of lymphocyte proliferation, differentiation, and survival. The regulatory activity is modulated by the state of differentiation of cells, the presence of inflammatory cytokines and costimulatory molecules. In addition, TGF-β promotes differentiation to $CD4^+CD25^+$ Tregs, which are key regulator of the immune tolerance. In terms of innate immunity, TGF-β controls homeostasis acting as a potent inhibitor of cytolytic activity of NK cells by downregulating the expression of activating receptors, and the production of IFN-γ (Li, Wan et al., 2006). This anti-inflammatory context mediated by the TGF-β signaling pathway is Smad2/3 dependent (canonical pathway). Conversely, TGF-β can regulate downstream cellular responses via other signal transducers in a context-dependent manner. Among the non-Smad TGF-β signaling pathways are the ERK1/2 pathway, P38/JNK and NFκB pathway (via TAK1), PI3K/AKT/mTOR pathway, MAP kinase pathway, JAK/STAT pathway, and the Rho-(like) GTPase pathway. Many of these signaling pathways are involved in various cellular processes such as inflammation, cell differentiation, and apoptosis (Tzavlaki & Moustakas, 2020).

BAMBI is a transmembrane protein structurally related to the TGF-β type I receptor superfamily. BAMBI mainly has TGF-β-mediated signaling inhibitory activity. It also inhibits BMP and activin-mediated signaling pathways. BAMBI is not essential for embryonic development and mice deficient in this protein do not have a macroscopically altered phenotype. However, studies performed by our group have reported that the absence of BAMBI in mice produces age-dependent thymic atrophy (unpublished data). In addition, the BAMBI deficiency or pharmacological inhibition with a monoclonal antibody promotes differentiation to Tregs, which produces protection against certain autoimmune and chronic inflammatory diseases (Alvarez et al., 2020; Postigo et al., 2016). This protective function is due to the essential role of BAMBI determining the strength of TGF-β signaling in murine CD4+ cells which ultimately regulates their functional differentiation into Th17 and Treg cells. The present study is focused on defining the link between the absence of BAMBI and the state of peripheral lymphocytes in homeostasis which supports the protective effect under pathologic conditions. Therefore, we have functionally characterized the peripheral immune cells of BAMBI-KO mice under homeostatic conditions at different points.

Although BAMBI-KO mice have a lower number of cells in the thymus and the number of lymphocytes migrating to the periphery is reduced, the total number of cells in the spleen did not show significant alterations. These results correlate with other studies that have not find alterations in the number of splenocytes in mice with a specific depletion in the TGF-β type II receptor in NK cells (Viel et al., 2016). Similarly, the total

number of CD4+ and CD8+ T lymphocytes in this organ did not have difference with WT mice. This pattern was also observed in T cell-specific Smad2/3 conditional KO mice with the canonical TGF-β signaling inhibited (Takimoto et al., 2010). In contrast, in a study using a murine model with no expression of TGF-β receptor II gene in T cells, increased number of both CD4+ and CD8+ T cells were observed (Li, Sanjabi, et al., 2006). Unlike T cells, NK cells showed an increase in the total number of cells in the spleen of 1- and 2-months old BAMBI-KO mice. However, these differences are not observed in older mice as reported by Viel and collaborators in mice with a specific depletion in the TGF-β type II receptor in these cells (Viel et al., 2016).

Since the absence of BAMBI seems to generate limited alterations in the abundance of lymphocytes populations, we further characterized mature and activated lymphocytes by the analysis of the expression of surface markers by flow cytometry. Both CD4+ and CD8+ T lymphocytes showed more $CD62L^{-}CD44^{+}$ effector memory phenotype in BAMBI-KO mice. Additionally, increased percentage of $CD27^{-}CD11b^{+}$ mature NK cells were found in BAMBI-KO mice. This cell pattern was accompanied by a decrease in the percentage of $CD62L^{+}CD44^{-}$ *naïve* T cells and $CD27^{+}CD11b^{-}$ immature NK cells. These results showing activated and mature peripheral lymphocytes in absence of BAMBI are apparently contradictory with the suppressive profile observed *in vivo*. In fact, increased ratio of effector memory: *naïve* cells were observed in CD4+ T cells from T cell-specific Smad2/3 conditional KO mice in which the canonical TGF-β signaling pathway was blocked (Takimoto et al., 2010). The phenotype of activated cells was also reported in CD8+ T cells from mice where the TGF-β signaling pathway was inhibited (Gu et al., 2012; N. Zhang & Bevan, 2012). Maturation pattern in NK cells from mice lacking TGF-β receptor-mediated signaling is more controversial since the differences observed by Marcoe et al. have been no reported by Viel et al (Marcoe et al., 2012; Viel et al., 2016). In contrast, we propose here an alternative hypothesis describing BAMBI as a unique rheostat that instead of a switch on/off mechanism, is capable to modulate multiple different levels of TGF-β signaling. Based on this singular property, BAMBI can promote not only either Treg or Th17 differentiation, but also a balance of suppressive versus activated immune cells.

To evaluate whether the expansion of mature and activated peripheral lymphocytes correlates with functional and proliferative capacities, we performed a proliferation assay *in vitro* of CD4+ and CD8+ T. Both CD4+ and CD8+ T cells from BAMBI-KO mice showed increased proliferation *in vitro* compared to WT T cells, with a proliferation rate of 1,56 (±0,08) and 1,78 (±0,17) respectively. In an *in vivo* study, it has been reported an increased proliferation of peripheral CD4+ and CD8+ T cells when TGF-β receptor signaling was deleted (Li, Sanjabi et al., 2006). In the same way,

splenocytes from *tgfb1*$^{-/-}$ mice showed a higher proliferative response *in vitro* (Bommireddy et al., 2003). The functionality of peripheral NK cells from BAMBI-KO mice has also been studied with a cytotoxicity assay *in vitro*. NK cells from BAMBI-KO mice had a higher cytotoxic activity and a higher expression of Granzyme B compared to WT cells. This higher expression of Granzyme B in NK cells was also observed in mice with a specific deletion of the TGF-β type II receptor gene in NK cells (Viel et al., 2016). However, a blockade of the BMP signaling pathway in NK cells by DMH1 (inhibitor of BMPs and activin receptors) produces a significant decrease in NK cell-mediated cytotoxicity *in vitro* (Robson et al., 2014). Taken together, these functional assays support our previous results where BAMBI deficiency promotes an activated and mature state in peripheral lymphocytes. Although these data confront most of the studies describing immune activation by blocking TGF-β signaling, they are in consonance with previous results from our lab showing B cell activation and antibodies production in BAMBI-KO mice. This regulation of the humoral response is TGF-β dependent, specifically involving non-canonical pathways through TAK1 (Augustín Rodríguez, 2017).

In conclusion, our results demonstrate high functional and activated phenotype of peripheral immune cells from BAMBI-KO mice under homeostatic conditions. These findings allow us to advance our knowledge about the role of BAMBI in the immune system. However, since the molecular pathways are still unknown, new studies will be required to characterize the specific involvement of TGF-β signaling including Smad dependent and independent pathways. The final goal will be to fully understand the mechanisms behind the role of BAMBI not only as a key regulator of tolerance but also, as a modulator of effective and mature immune cells.

6. Conclusions.

- Although our previous results show that the absence of BAMBI under homeostatic conditions reduces the number of thymocytes, the total number of splenocytes is not altered.
- Splenic CD4+ and CD8+ T cells from BAMBI deficient mice show no change in cell viability whereas both present more proliferative ability. This expansion may explain that lower generation of T cells in the thymus does not affect the number of peripheral T lymphocytes.
- BAMBI-KO mice present higher proportion of mature and activated peripheral lymphocytes under homeostatic conditions while these mice have shown protection against autoimmune and chronic inflammatory diseases.
- The absence of BAMBI produces an increase in the cytotoxic capacity of stimulated NK cells, which correlates with higher production of Granzyme B becoming a very promising model for new therapeutic targets.

7. Bibliography.

Akhurst, R. J., & Hata, A. (2012). **Targeting the TGFβ signalling pathway in disease**. *Nature Reviews Drug Discovery*, *11*(10), 790–811.

Alvarez, P., Augustín, J. J., Tamayo, E., Iglesias, M., Acinas, O., Mendiguren, M. A., Vázquez, J. A., Genre, F., San Segundo, D., Merino, J., & Merino, R. (2020). **Therapeutic Effects of Anti–Bone Morphogenetic Protein and Activin Membrane-Bound Inhibitor Treatment in Psoriasis and Arthritis**. *Arthritis & Rheumatology*, *72*(9), 1547–1558.

Andoniou, C. E., van Dommelen, S. L. H., Voigt, V., Andrews, D. M., Brizard, G., Asselin-Paturel, C., Delale, T., Stacey, K. J., Trinchieri, G., & Degli-Esposti, M. A. (2005). **Interaction between conventional dendritic cells and natural killer cells is integral to the activation of effective antiviral immunity**. *Nature Immunology*, *6*(10), 1011–1019.

Augustín Rodríguez, J. J. (2017). **The role of BAMBI in the regulation of the humoral immune response**. University of Cantabria.

Bettelli, E., Carrier, Y., Gao, W., Korn, T., Strom, T. B., Oukka, M., Weiner, H. L., & Kuchroo, V. K. (2006). **Reciprocal developmental pathways for the generation of pathogenic effector TH17 and regulatory T cells**. *Nature*, *441*(7090), 235–238.

Bommireddy, R., Saxena, V., Ormsby, I., Yin, M., Boivin, G. P., Babcock, G. F., Singh, R. R., & Doetschman, T. (2003). **TGF-β1 Regulates Lymphocyte Homeostasis by Preventing Activation and Subsequent Apoptosis of Peripheral Lymphocytes**. *The Journal of Immunology*, *170*(9), 4612–4622.

Borghesi, L., Hsu, L.-Y., Miller, J. P., Anderson, M., Herzenberg, L., Herzenberg, L., Schlissel, M. S., Allman, D., & Gerstein, R. M. (2004). **B Lineage–specific Regulation of V(D)J Recombinase Activity Is Established in Common Lymphoid Progenitors**. *The Journal of Experimental Medicine*, *199*(4), 491–502.

Boyman, O., & Sprent, J. (2012). **The role of interleukin-2 during homeostasis and activation of the immune system**. *Nature Reviews Immunology*, *12*(3), 180–190.

Calabro, S., Liu, D., Gallman, A., Nascimento, M. S. L., Yu, Z., Zhang, T., Chen, P., Zhang, B., Xu, L., Gowthaman, U., Krishnaswamy, J. K., Haberman, A. M., Williams, A., & Eisenbarth, S. C. (2016). **Differential Intrasplenic Migration of Dendritic Cell Subsets Tailors Adaptive Immunity**. *Cell Reports*, *16*(9), 2472–2485.

Chen, X., Li, J., Xiang, A., Guan, H., Su, P., Zhang, L., Zhang, D., & Yu, Q. (2023). **BMP and activin receptor membrane bound inhibitor: BAMBI has multiple roles in gene expression and diseases**. *Experimental and Therapeutic Medicine*, *27*(1), 28.

Cox, M. A., Kahan, S. M., & Zajac, A. J. (2013). **Anti-viral CD8 T cells and the cytokines that they love**. *Virology*, *435*(1), 157–169.

Di Santo, J. P. (2006). **Natural Killer cell developmental pathways: a question of balance**. *Annual Review of Immunology*, *24*(1), 257–286.

Fabbri, M. (2003). **T lymphocytes**. *The International Journal of Biochemistry & Cell Biology*, *35*(7), 1004–1008.

Gu, A.-D., Wang, Y., Lin, L., Zhang, S. S., & Wan, Y. Y. (2012). **Requirements of transcription factor Smad-dependent and -independent TGF-β signaling to control discrete T-cell functions**. *Proceedings of the National Academy of Sciences*, *109*(3), 905–910.

Hartsough, M. T., & Mulder, K. M. (1995). **Transforming Growth Factor β Activation of p44mapk in Proliferating Cultures of Epithelial Cells**. *Journal of Biological Chemistry*, *270*(13), 7117–7124.

Huntington, N. D., Puthalakath, H., Gunn, P., Naik, E., Michalak, E. M., Smyth, M. J., Tabarias, H., Degli-Esposti, M. A., Dewson, G., Willis, S. N., Motoyama, N., Huang, D. C. S., Nutt, S. L., Tarlinton, D. M., & Strasser, A. (2007). **Interleukin 15-mediated survival of natural killer cells is determined by interactions among Bim, Noxa and Mcl-1**. *Nature Immunology*, *8*(8), 856–863.

Jung, D., Baek, Y. S., Lee, I. J., Kim, K. Y., Jang, H., Hwang, S., Jung, J., Moon, Y., Park, K.-S., Choi, Y.-S., & An, H. J. (2021). **Ex vivo expanded allogeneic natural killer cells have potent cytolytic activity against cancer cells through different receptor-ligand interactions**. *Journal of Experimental & Clinical Cancer Research*, *40*(1), 333.

Klein, L., Kyewski, B., Allen, P. M., & Hogquist, K. A. (2014). **Positive and negative selection of the T cell repertoire: what thymocytes see (and don't see)**. *Nature Reviews Immunology*, *14*(6), 377–391.

Kumar, B. V., Connors, T. J., & Farber, D. L. (2018). **Human T Cell Development, Localization, and Function throughout Life**. *Immunity*, *48*(2), 202–213.

Li, M. O., Sanjabi, S., & Flavell, R. A. (2006). **Transforming Growth Factor-β Controls Development, Homeostasis, and Tolerance of T Cells by Regulatory T Cell-Dependent and -Independent Mechanisms**. *Immunity*, *25*(3), 455–471.

Li, M. O., Wan, Y. Y., Sanjabi, S., Robertson, A.-K. L., & Flavell, R. A. (2006). **Transforming Growth Factor-β Regulation of Immune Responses**. *Annual Review of Immunology*, *24*(1), 99–146.

Liu, K., Song, X., Ma, H., Liu, L., Wen, X., Yu, J., Wang, L., & Hu, S. (2014). **Knockdown of BAMBI inhibits β-catenin and transforming growth factor β to suppress metastasis of gastric cancer cells**. *Molecular Medicine Reports*, *10*(2), 874–880.

Ljunggren, H.-G., & Kärre, K. (1990). **In search of the 'missing self': MHC molecules and NK cell recognition**. *Immunology Today*, *11*, 237–244.

Lu, E., Dang, E. V., McDonald, J. G., & Cyster, J. G. (2017). **Distinct oxysterol requirements for positioning naïve and activated dendritic cells in the spleen**. *Science Immunology*, *2*(10).

Malek, T. R., & Bayer, A. L. (2004). **Tolerance, not immunity, crucially depends on IL-2**. *Nature Reviews Immunology*, *4*(9), 665–674.

Marcoe, J. P., Lim, J. R., Schaubert, K. L., Fodil-Cornu, N., Matka, M., McCubbrey, A. L., Farr, A. R., Vidal, S. M., & Laouar, Y. (2012). **TGF-β is responsible for NK cell immaturity during ontogeny and increased susceptibility to infection during mouse infancy**. *Nature Immunology*, *13*(9), 843–850.

Mebius, R. E., & Kraal, G. (2005). **Structure and function of the spleen**. *Nature Reviews Immunology*, *5*(8), 606–616.

Mulder, K. M., & Morris, S. L. (1992). **Activation of p21ras by transforming growth factor beta in epithelial cells**. *Journal of Biological Chemistry*, *267*(8), 5029–5031.

Postigo, J., Iglesias, M., Álvarez, P., Jesús Augustin, J., Buelta, L., Merino, J., & Merino, R. (2016). **Bone Morphogenetic Protein and Activin Membrane–Bound Inhibitor, a Transforming Growth Factor β Rheostat That Controls Murine Treg Cell/Th17 Cell Differentiation and the Development of Autoimmune Arthritis by Reducing Interleukin-2 Signaling.** *Arthritis & Rheumatology*, *68*(6), 1551–1562.

Robson, N. C., Hidalgo, L., McAlpine, T., Wei, H., Martínez, V. G., Entrena, A., Melen, G. J., MacDonald, A. S., Phythian-Adams, A., Sacedón, R., Maraskovsky, E., Cebon, J., Ramírez, M., Vicente, A., & Varas, A. (2014). **Optimal Effector Functions in Human Natural Killer Cells Rely upon Autocrine Bone Morphogenetic Protein Signaling**. *Cancer Research*, *74*(18), 5019–5031.

Seki, E., De Minicis, S., Österreicher, C. H., Kluwe, J., Osawa, Y., Brenner, D. A., & Schwabe, R. F. (2007). **TLR4 enhances TGF-β signaling and hepatic fibrosis**. *Nature Medicine*, *13*(11), 1324–1332.

Sekiya, T., Adachi, S., Kohu, K., Yamada, T., Higuchi, O., Furukawa, Y., Nakamura, Y., Nakamura, T., Tashiro, K., Kuhara, S., Ohwada, S., & Akiyama, T. (2004). **Identification of BMP and Activin Membrane-bound Inhibitor (BAMBI), an Inhibitor of Transforming Growth Factor-β Signaling, as a Target of the β-Catenin Pathway in Colorectal Tumor Cells**. *Journal of Biological Chemistry*, *279*(8), 6840–6846.

Sekiya, T., Oda, T., Matsuura, K., & Akiyama, T. (2004). **Transcriptional regulation of the TGF-β pseudoreceptor BAMBI by TGF-β signaling**. *Biochemical and*

Biophysical Research Communications, *320*(3), 680–684.

Steiniger, B., & Barth, P. (2000). **Microanatomy and function of the spleen**. *Advances in Anatomy, Embryology, and Cell Biology*, *151*, III–IX, 1–101.

Sun, S.-W., Chen, L., Zhou, M., Wu, J.-H., Meng, Z.-J., Han, H.-L., Miao, S.-Y., Zhu, C.-C., & Xiong, X.-Z. (2019). **BAMBI regulates macrophages inducing the differentiation of Treg through the TGF-β pathway in chronic obstructive pulmonary disease**. *Respiratory Research*, *20*(1), 26.

Takimoto, T., Wakabayashi, Y., Sekiya, T., Inoue, N., Morita, R., Ichiyama, K., Takahashi, R., Asakawa, M., Muto, G., Mori, T., Hasegawa, E., Shizuya, S., Hara, T., Nomura, M., & Yoshimura, A. (2010). **Smad2 and Smad3 Are Redundantly Essential for the TGF-β–Mediated Regulation of Regulatory T Plasticity and Th1 Development**. *The Journal of Immunology*, *185*(2), 842–855.

Tramullas, M., Lantero, A., Díaz, Á., Morchón, N., Merino, D., Villar, A., Buscher, D., Merino, R., Hurlé, J. M., Izpisúa-Belmonte, J. C., & Hurlé, M. A. (2010). **BAMBI (Bone Morphogenetic Protein and Activin Membrane-Bound Inhibitor) Reveals the Involvement of the Transforming Growth Factor-β Family in Pain Modulation**. *The Journal of Neuroscience*, *30*(4), 1502–1511.

Tzavlaki, K., & Moustakas, A. (2020). **TGF-β Signaling**. *Biomolecules*, *10*(3), 487.

Viel, S., Marçais, A., Guimaraes, F. S.-F., Loftus, R., Rabilloud, J., Grau, M., Degouve, S., Djebali, S., Sanlaville, A., Charrier, E., Bienvenu, J., Marie, J. C., Caux, C., Marvel, J., Town, L., Huntington, N. D., Bartholin, L., Finlay, D., Smyth, M. J., & Walzer, T. (2016). **TGF-β inhibits the activation and functions of NK cells by repressing the mTOR pathway**. *Science Signaling*, *9*(415).

Viret, C., & Janeway, C. A. (1999). **MHC and T cell development**. *Reviews in Immunogenetics*, *1*(1), 91–104.

Wong, P., Wagner, J. A., Berrien-Elliott, M. M., Schappe, T., & Fehniger, T. A. (2021). **Flow cytometry-based ex vivo murine NK cell cytotoxicity assay**. *STAR Protocols*, *2*(1), 100262.

Yan, X., Lin, Z., Chen, F., Zhao, X., Chen, H., Ning, Y., & Chen, Y.-G. (2009). **Human BAMBI Cooperates with Smad7 to Inhibit Transforming Growth Factor-β Signaling**. *Journal of Biological Chemistry*, *284*(44), 30097–30104.

Zhang, J.-C., Chen, G., Chen, L., Meng, Z.-J., Xiong, X.-Z., Liu, H.-J., Jin, Y., Tao, X.-N., Wu, J.-H., & Sun, S.-W. (2016). **TGF-β/BAMBI pathway dysfunction contributes to peripheral Th17/Treg imbalance in chronic obstructive pulmonary disease**. *Scientific Reports*, *6*(1), 31911.

Zhang, N., & Bevan, M. J. (2012). **TGF-β signaling to T cells inhibits autoimmunity during lymphopenia-driven proliferation**. *Nature Immunology*, *13*(7), 667–673.